POLITECNICO DI MILANO
Dipartimento di Chimica Materiali e Ingegneria Chimica
"Giulio Natta"

ADVANCED APPROACHES TO THE KINETIC STUDY OF CATALYTIC REACTIONS:

a) Transient methods;
b) Structured lab-scale reactors.

EUROKIN
Billingham – UK
June 26th, 2003

Enrico Tronconi

Outline (1/2)

1. **Transient Response Methods applied to the kinetic analysis of the DeNOx-SCR reaction**

- Transient adsorption-desorption and reactivity study of the SCR reactants (NH_3, NO) over $V/W/TiO_2$ catalysts
- Kinetic modeling and comparison with steady-state data
- Role of WO_3, kinetic influence of H_2O
- Application to dynamic modeling of SCR reactors

- Extension of TRMs to the kinetic analysis of NOx storage in NOx traps ($Pt/BaO/Al_2O_3$ systems)

Outline (2/2)

2. Lab-scale structured reactors for kinetic measurements in catalytic combustion

- ✓ Design and operation of an **annular reactor** for the kinetic study of CH_4 catalytic combustion
  - Modeling
  - Minimizing the impact of transport limitations
  - Kinetic results over $Pd/\gamma Al_2O_3$
- ✓ Application of a **metallic plate-type reactor** to the kinetic study of CO catalytic oxidation
  - Use heat conduction to effectively remove the reaction heat
  - Experimental results over $Pd/\gamma Al_2O_3$ coated Al slabs
  - Kinetic analysis

Debated Issues in SCR-DeNOx Catalysis over $V_2O_5/WO_3/TiO_2$ Systems

$$4\ NO + 4\ NH_3 + O_2 \rightarrow 4\ N_2 + 6\ H_2O$$

- ER vs. LH mechanism? Adsorption vs. active sites?
- Rate determining step? Steady-state rate expression:

$$r_{NO} = k_{NO} C_{NO} \frac{K_{NH3} C_{NH3}}{1 + K_{NH3} C_{NH3}} ?$$

- Promoting role of WO_3?
- Inhibiting action of H_2O due to competitive adsorption with NH_3?

Transient Response Methods

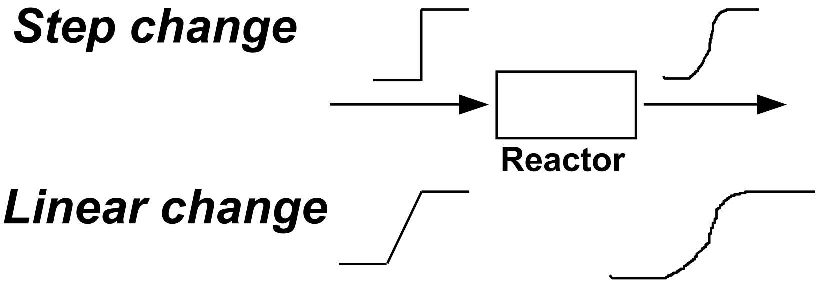

Step change

Reactor

Linear change

- The reacting system is perturbed (e.g. by changes of the feed composition), and its transient response is recorded.
- The response (e.g. the outlet composition) reflects the characteristics of the elementary steps in the kinetic sequence of the reaction.
- The elementary steps do not proceed at the same rate.

SCR Transient Response Experiments

Approach

- Transient adsorption-desorption study of the individual SCR reactants (NH_3, NO) over $V/W/TiO_2$
  - NH_3, NO adsorption onto model and commercial catalysts
  - NH_3 oxidation
- Transient reactivity study (NH_3 + NO)
  - stepwise and linear changes of NH_3 in NO continuous flow
  - stepwise and linear changes of NO in NH_3 continuous flow

Rigs for Transient Response Experiments at PoliMI

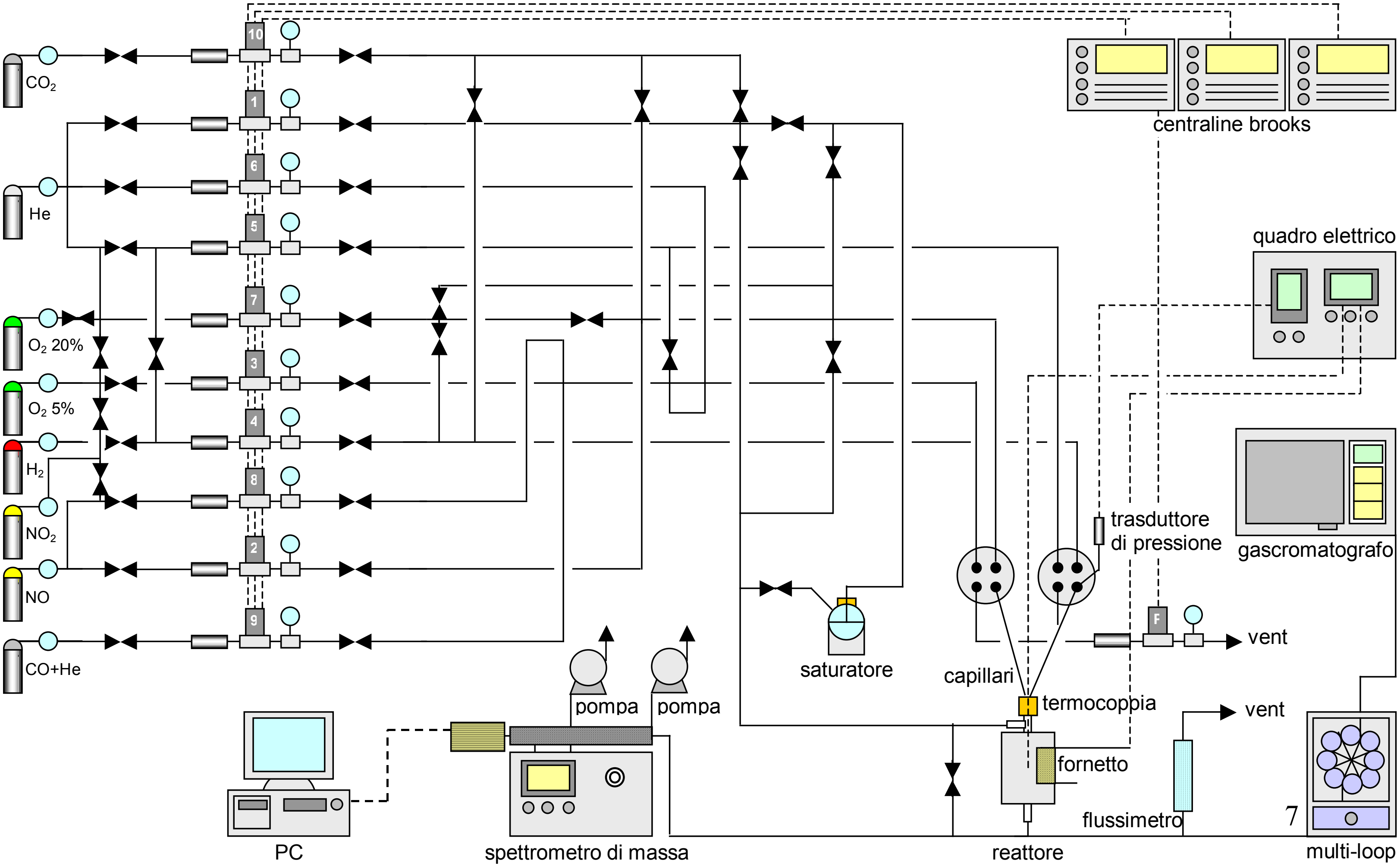

SCR Transient Response Experiments

Experimental Details

- Catalysts :
  - model [V_2O_5(1.47%)/TiO_2 and V_2O_5(1.47%)/WO_3(9%)/TiO_2]
  - commercial [V_2O_5(0.62%)/WO_3(9%)/TiO_2]
- Reactor:
  - W_{cat} = 0.12 - 0.16 g; d_p = 100 micron;
  - d_t = 0.6 cm; L_b = 1 cm
- Operating conditions:
  - Q = 120 – 280 Ncm^3/min
  - GHSV = 45000 – 140000 h^{-1}
  - C - ramp = 20 ppm/min

Transient Adsorption-desorption Study

NH_3 Adsorption-desorption

Step change of the NH_3 inlet concentration

in He + O_2 (1%); Model V_2O_5-WO_3/TiO_2 catalyst; T = 280°C

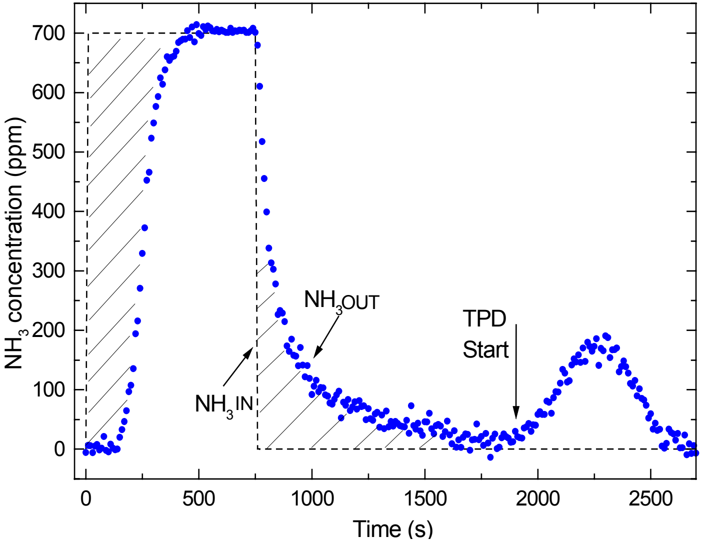

Linear change of the NH_3 inlet concentration

in He + O_2 (2%); Commercial V_2O_5-WO_3/TiO_2 catalyst; T = 300°C

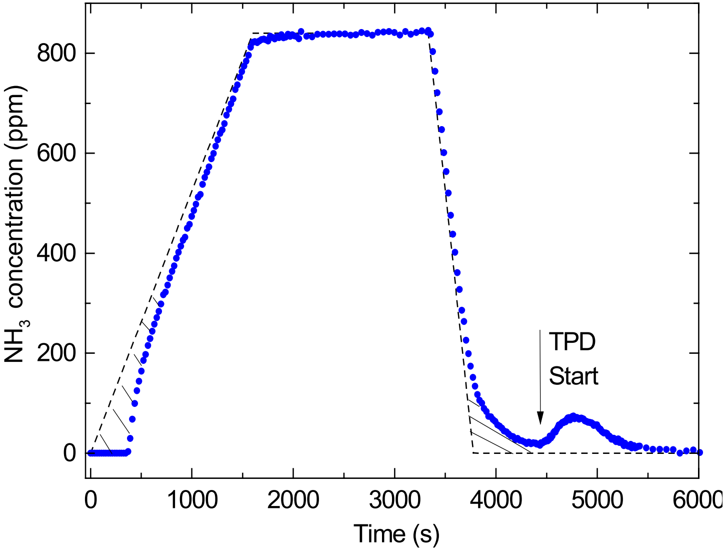

Transient Adsorption-desorption Study

NH_3 Adsorption-desorption – Effect of Temperature

Step change of C°NH_3

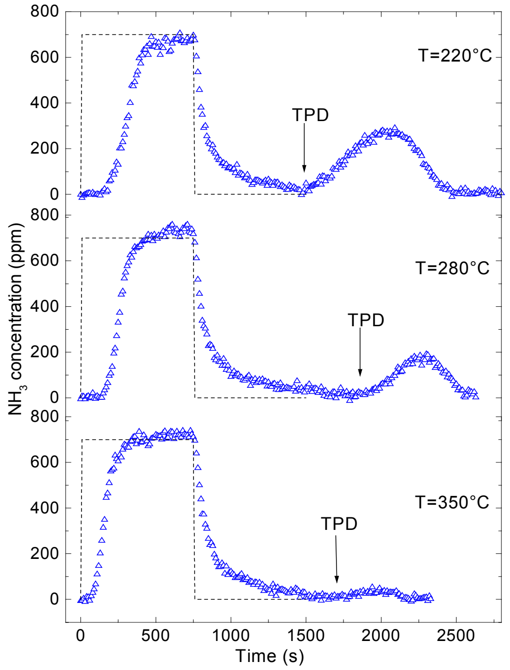

Linear change of C°NH_3

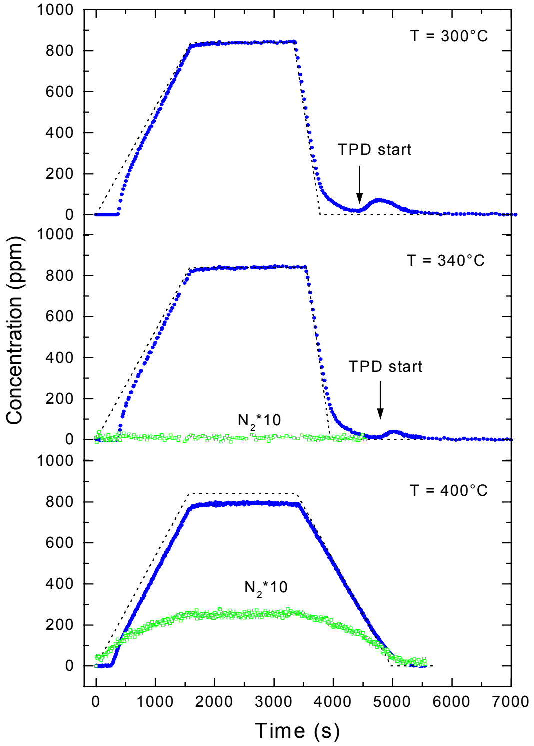

Transient Adsorption-desorption Study

NO Adsorption-desorption

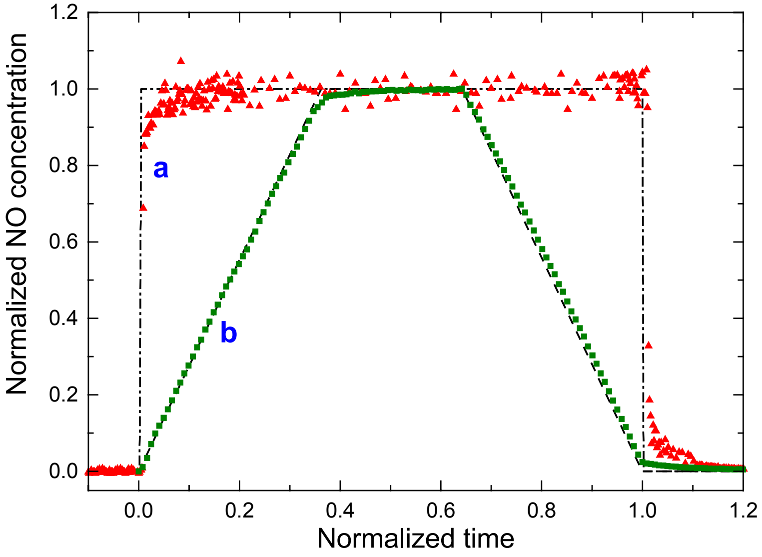

a) Step change of NO inlet concentration. Model ternary catalyst, T = 280 °C

b) Linear change, commercial catalyst, T = 300 °C

Kinetic analysis of NH_3 Adsorption-desorption 1D Heterogeneous Isothermal PFR Model

- NH_3 mass balance, catalyst:

$$\frac{\partial \theta_{NH3}}{\partial t} = r_{ad} - r_{des} - r_{ox}$$

- NH_3 and N_2 mass balances, gas phase:

$$\frac{\partial C_{NH3}}{\partial t} = -v \cdot \frac{\partial C_{NH3}}{\partial z} - \Omega \cdot (r_{ad} - r_{des})$$

$$\frac{\partial C_{N2}}{\partial t} = -v \cdot \frac{\partial C_{N2}}{\partial z} + \Omega \cdot 0.5 \cdot r_{ox}$$

- Rate equations for NH_3 adsorption, desorption and oxidation:

$$r_{ads} = k_{ads} C_{NH_3} \left(1 - \theta_{NH_3}\right)$$

$$r_{des} = k^{\circ}_{des} \exp\left[-\frac{E^{\circ}_{des}}{RT}\left(1 - \alpha\theta_{NH_3}\right)\right] \cdot \theta_{NH_3}$$

$$r_{ox} = k_{ox} \cdot \theta_{NH3}$$

Kinetic analysis of NH_3 Adsorption-desorption Data Fit

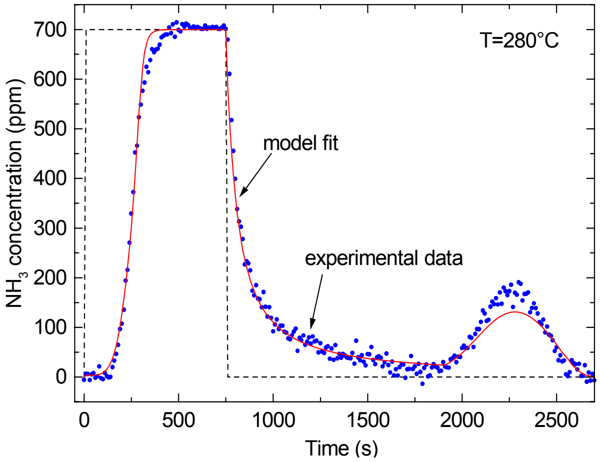

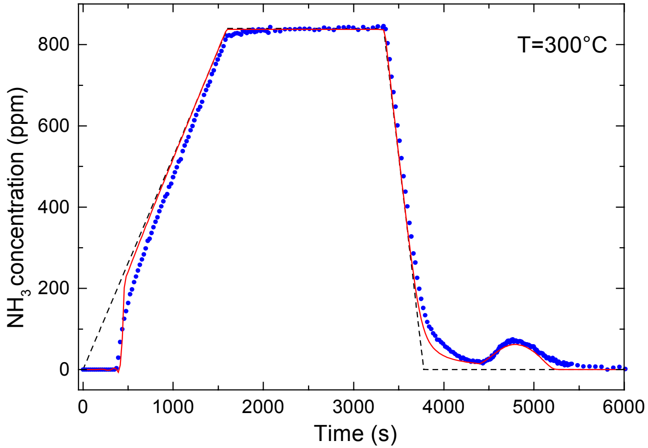

Step change of the NH_3 inlet concentration in He + O_2.
Model V_2O_5-WO_3/TiO_2 catalyst
Kinetic parameters: $k°_a$=0.487 m^3/mol s, $k°_d$=2.67 E+5 1/s, $E°_d$= 22.9 kcal/mol, α=0.405, Ω_{NH3}=270 mol/m^3

Linear variation of the NH_3 inlet concentration in He + O_2.
Commercial WO_3-V_2O_5/TiO_2 catalyst.
Kinetic parameters: $k°_a$= 33.87 m^3/mol s, $k°_d$=2.2 E+6 1/s, $E°_d$= 23.0 kcal/mol, α=0.256, Ω_{NH3}=270 mol/m^3

Kinetic analysis of NH_3 Adsorption-desorption NH_3 Oxidation

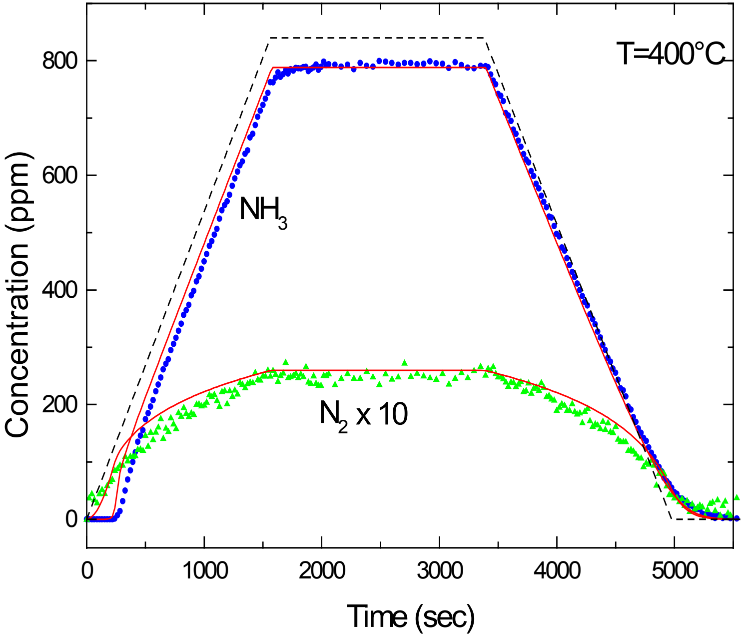

Linear change of the NH_3 inlet concentration in He + O_2.
Commercial V_2O_5-WO_3/TiO_2 catalyst

Kinetic parameters:

$k°_{ox} = 3.25 \times 10^6$ 1/s,

$E°_{ox} = 28.8$ kcal/mol

Transient NH_3 + NO Reactivity Study

NH_3 variations in constant NO flow

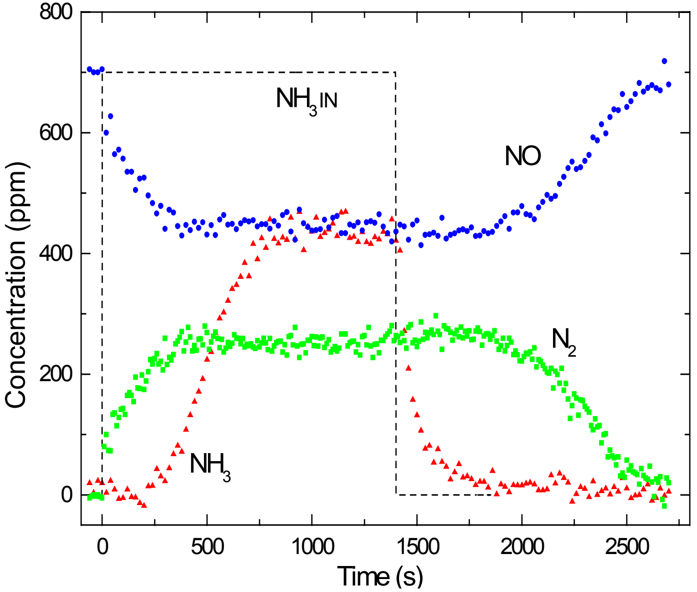

NH_3 step change

in He + O_2 (1% v/v)+NO (700 ppm)
Model WO_3-V_2O_5/TiO_2 catalyst
T=220°C, GHSV = 75000 h^{-1}

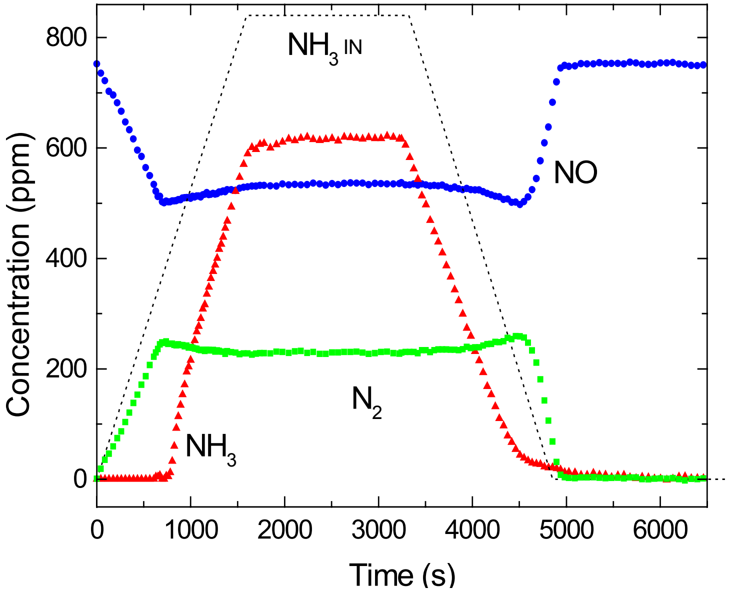

NH_3 linear change

in He + O_2 (2% v/v)+NO (750 ppm)
Commercial WO_3-V_2O_5/TiO_2 catalyst
T=300°C, GHSV = 140000 h^{-1}

Transient NH_3 + NO Reactivity Study

NO variations in constant NH_3 flow

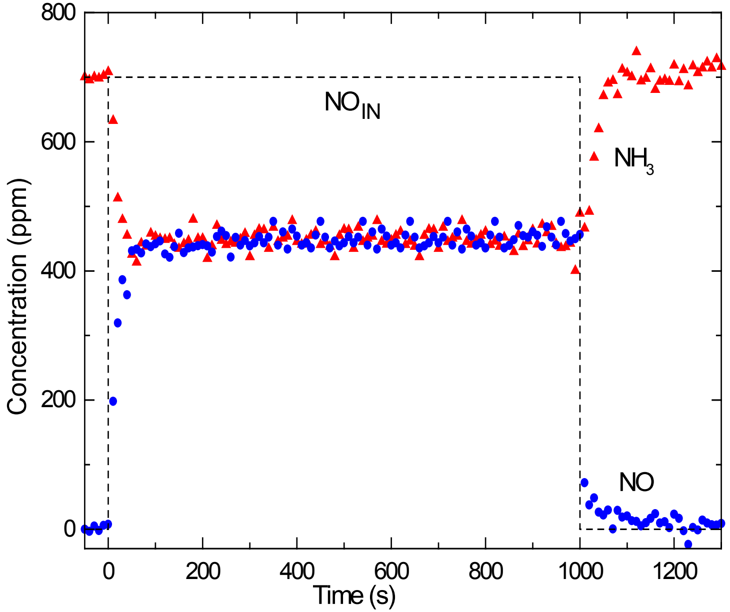

NO step change

in He + O_2 (1% v/v) + NH_3 (700ppm)
Model WO_3-V_2O_5/TiO_2 catalyst
T=220°C, GHSV = 45000 h^{-1}

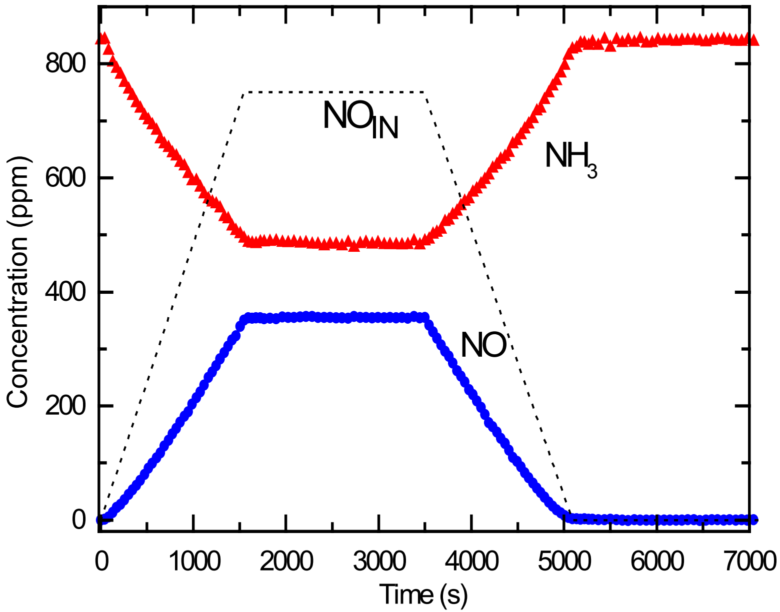

NO linear change

in He + O_2 (2 % v/v) +NH_3 (840 ppm)
Commercial WO_3-V_2O_5/TiO_2 catalyst
T=300°C, GHSV = 140000 h^{-1}

Transient Kinetic Analysis

Dual-site “NH_3 Reservoir” Kinetics

(1) $NH_3+T \underset{k_{des}}{\overset{k_{ads}}{\rightleftarrows}} [NH_3^*]_T$

(2) $[NH_3^*]_T+V \overset{K_{VT}}{\rightleftarrows} [NH_3^*]_V+T$

(3) $[NH_3^*]_V+NO \xrightarrow[+O_2]{k_{NO}} N_2+H_2O+V$

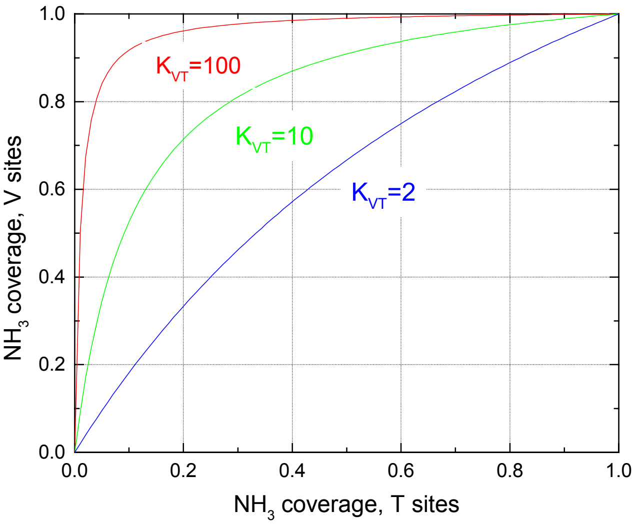

$$r_3 = k_{NO} C_{NO} \frac{K_{VT}\vartheta_{NH3,T}}{1+(K_{VT}-1)\vartheta_{NH3,T}}$$

Transient Kinetic Analysis

NH_3 changes in continuous NO flow: Data Fit

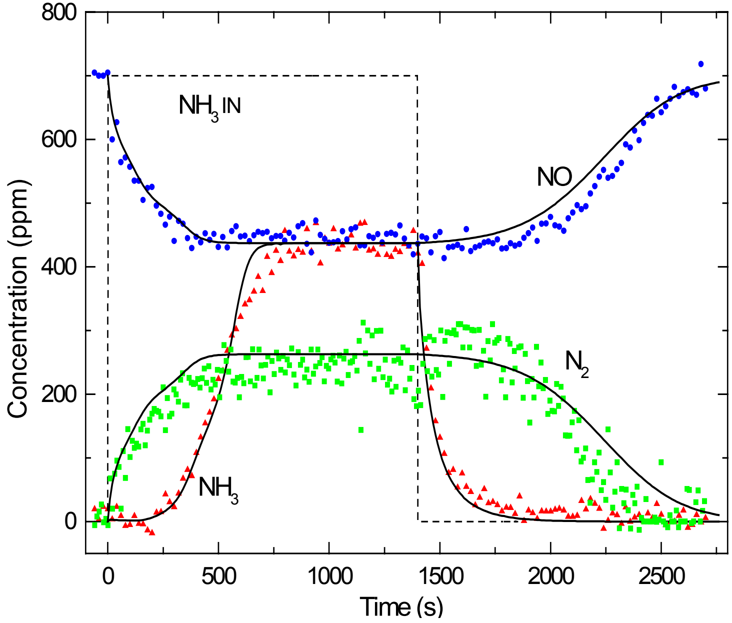

NH_3 step change in He + $O_{2.}$
Model V_2O_5-WO_3/TiO_2 catalyst
Kinetic parameters: k°$_{NO}$= 9.2×10^4 1/s,
E°$_{NO}$= 14.2 kcal/mol, K_{VT} = 12.4

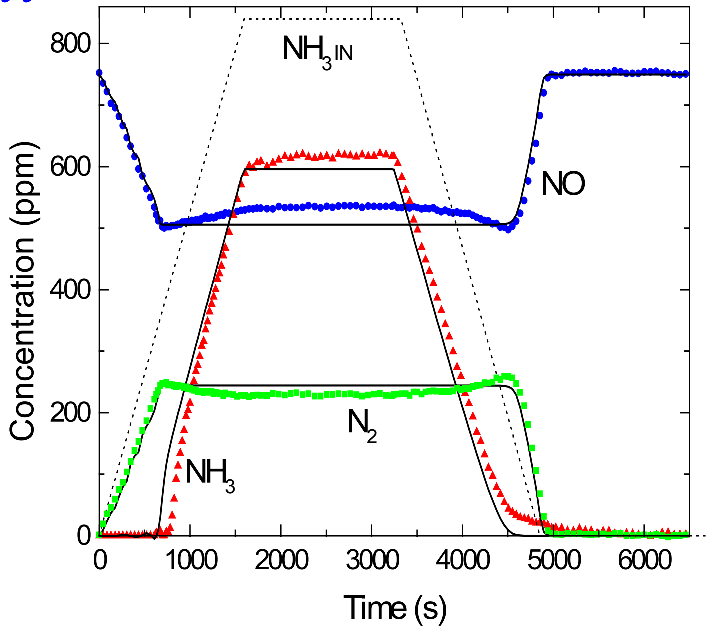

NH_3 linear variation in He + $O_{2.}$
Commercial WO_3-V_2O_5/TiO_2 catalyst.
Kinetic parameters: k°$_{NO}$= 7.1×10^6 1/s,
E°$_{NO}$= 19.2 kcal/mol, K_{VT} = 68.0

Transient Kinetic Analysis

NO changes in continuous NH_3 flow: Simulation

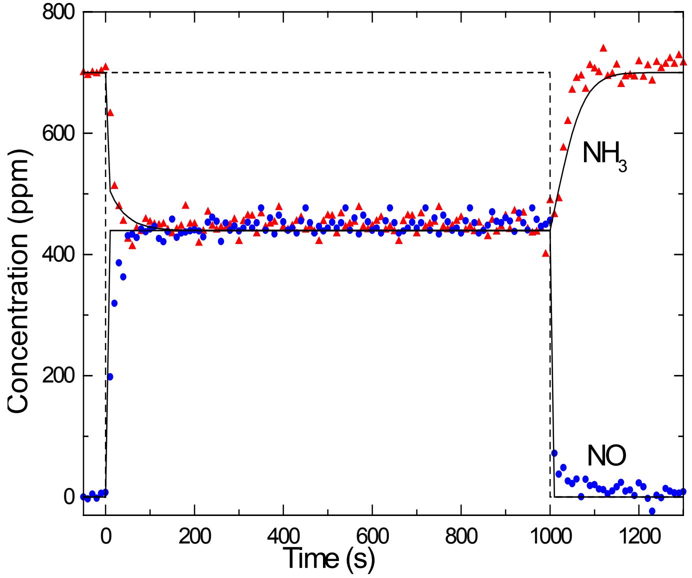

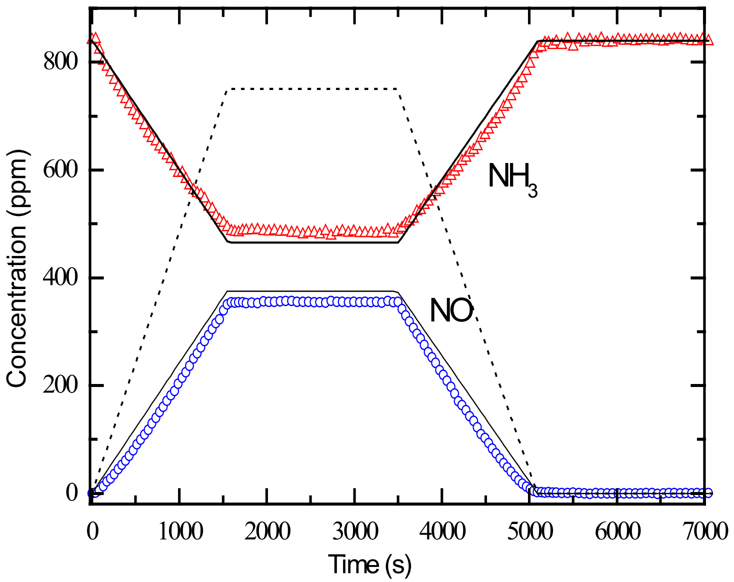

NO step change

in He + O_2 (1% v/v) + NH_3 (700ppm)
Model WO_3-V_2O_5/TiO_2 catalyst
T=220°C, GHSV = 75000 h^{-1}

NO linear variation

in He + O_2 (2 % v/v) +NH_3 (840 ppm)
Commercial WO_3-V_2O_5/TiO_2 catalyst
T=300°C, GHSV = 140000 h^{-1}

Transient Kinetic Analysis

Rate determining step at steady-state

$$NH_3 \underset{r_{des}}{\overset{r_{ads}}{\rightleftarrows}} NH_3^* \xrightarrow[+\,NO]{r_{NO}} N_2$$

Surface reaction = r.d.s. if: $\Phi = \dfrac{r_{ads}}{r_{NO}} >> 1$

Values of Φ (C_{NO}=500 ppm)	T = 300 °C	T = 340 °C	T = 380 °C
C_{NH3}=500 ppm	37.3	17.0	8.23
C_{NH3}=400 ppm	31.9	14.3	6.91
C_{NH3}=300 ppm	25.9	11.5	5.50

Role of WO_3

in NH_3 adsorption-desorption

NH_3 step change

in He + O_2 (1% v/v)

Model catalysts.

T=280°C, GHSV = 75000 h^{-1}

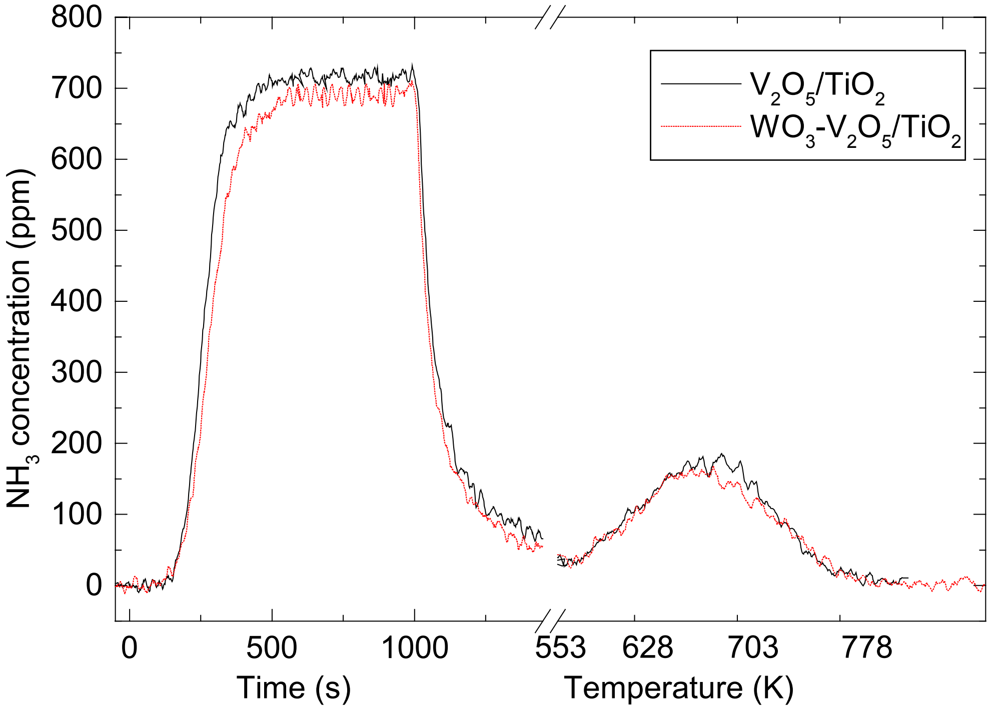

Role of WO_3

in NH_3 + NO reactivity

NH_3 step change

in He + O_2 (1% v/v) + NO (700 ppm)

Model catalysts.

T=280°C, GHSV = 75000 h^{-1}

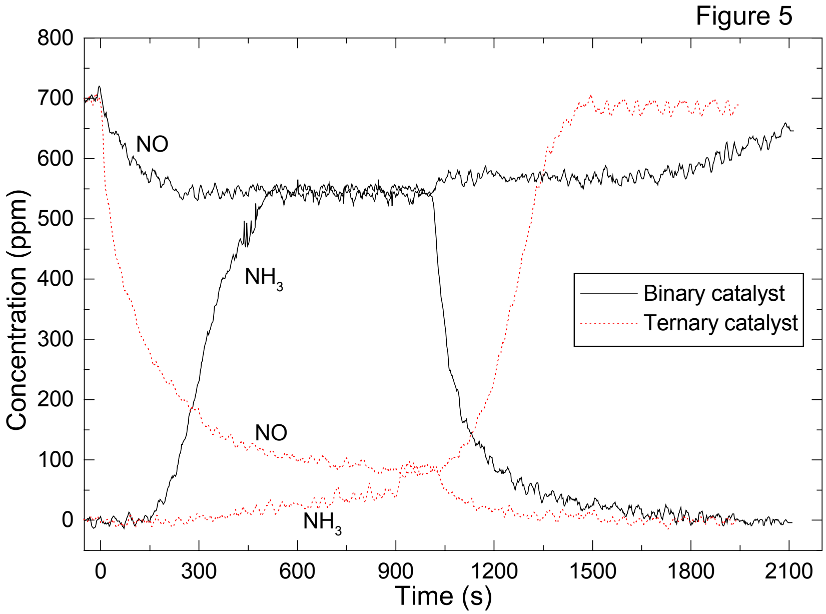

SCR Transient kinetic study: Conclusions

- NH_3 is strongly adsorbed onto $V_2O_5/WO_3/TiO_2$ catalysts, which work as "ammonia storage" systems
- NO is not appreciably adsorbed
- NH_3 adsorption-desorption rate was fitted by Temkin-type kinetics
- NO + NH_3 surface reaction rate was fitted according to dual-site "reservoir" kinetics
- The assumption of equilibrium NH_3 adsorption may be critical
- WO_3 does not affect NH_3 adsorption, but greatly promotes NO + NH_3 reactivity
- Inhibition by H_2O does not result from competitive adsorption with NH_3

Dynamic modeling of SCR-DeNOx monolith reactors

- Unsteady kinetics of DeNOx catalysis by Transient Response Methods (Lietti et al., AIChE J, 1996)
- Dynamic SCR monolith reactor model + validation (Tronconi et al., IEC Res., 1998)
- Inclusion of SO_2 oxidation (Tronconi et al., IEC Res., 1999)

Validation of the dynamic SCR monolith reactor model

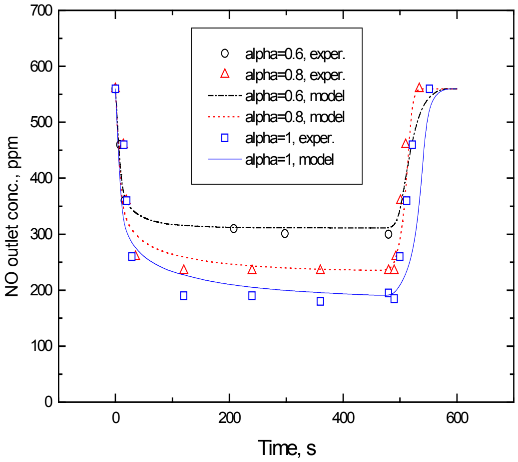

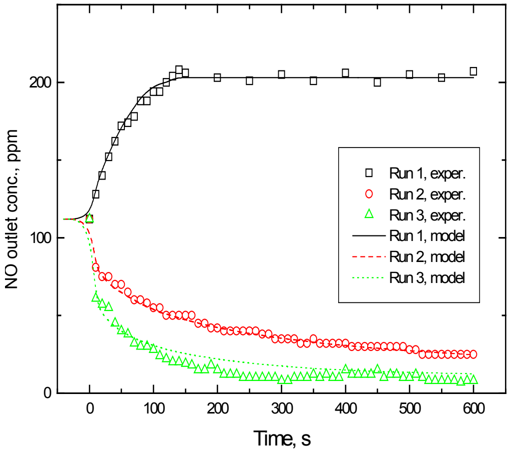

- Experimental and simulated evolutions of the NO outlet concentration during SCR reactor start-up and shut-down, and following step variations of NO inlet concentration

(Tronconi et al., Ind. Eng. Chem. Res, 1998)

Main literature references for transient SCR kinetics

L. Lietti, I. Nova, S. Camurri, E. Tronconi, P. Forzatti
"Study of the Dynamics of the SCR - DeNOx Reaction by the Transient Response Method"
AIChE J., 43, 2559-2570 (1997).

E. Tronconi, A. Cavanna, P. Forzatti
"Unsteady Analysis of NO Reduction over Selective Catalytic Reduction - De-NOx Monolith Catalysts"
Ind. Eng. Chem. Res., 37, 2341-2349 (1998).

E. Tronconi, C. Orsenigo, A. Cavanna, P. Forzatti
"Transient Kinetics of SO2 Oxidation over SCR-DeNOx Monolith Catalysts"
Ind. Eng. Chem. Res., 38, 2593-2598 (1999).

I. Nova, L. Lietti, E. Tronconi, P. Forzatti
"Transient response method applied to the kinetic analysis of the DeNOx-SCR reaction"
Chem. Eng. Sci., 56, 1229-1237 (2001).

Applying TRMs to study the kinetics of NOx storage in NOx traps (Pt/BaO/Al$_2$O$_3$ systems)

Elementary Steps

$$O_2 + 2Pt \underset{2}{\overset{1}{\rightleftharpoons}} 2Pt\text{-}O$$

$$NO + Pt \underset{4}{\overset{3}{\rightleftharpoons}} Pt\text{-}NO$$

$$NO_2 + Pt \underset{6}{\overset{5}{\rightleftharpoons}} Pt\text{-}NO_2$$

$$Pt\text{-}NO + Pt\text{-}O \underset{8}{\overset{7}{\rightleftharpoons}} Pt\text{-}NO_2 + Pt$$

Reactions over Pt

$$NO_2 + S \underset{10}{\overset{9}{\rightleftharpoons}} S\text{-}NO_2$$

$$S\text{-}NO_2 \underset{12}{\overset{11}{\rightleftharpoons}} S\text{-}O + NO$$

$$NO_2 + S\text{-}O \underset{14}{\overset{13}{\rightleftharpoons}} S\text{-}NO_3$$

$$NO_2 + S\text{-}NO_3 \underset{16}{\overset{15}{\rightleftharpoons}} Ba(NO_3)_2$$

$$2\,S\text{-}O \underset{18}{\overset{17}{\rightleftharpoons}} 2\,S + O_2$$

Reactions over BaO

$$Pt\text{-}NO_2 + S\text{-}NO_3 \underset{20}{\overset{19}{\rightleftharpoons}} Ba(NO_3)_2 + Pt$$

Spillover

Detailed kinetic scheme proposed by Olsson et al.,
J. Phys. Chem. 105 (2001) 6895 – 6906

adapted and compared to our TRM data, covering a variety of combinations of:

- catalytic systems (binary, ternary)
- feed compositions (NO, NO$_2$, O$_2$)

in order to test its physico-chemical consistency

TRM - Experimental

Adsorption + TPD

- NO_x storage phase
- Temperature programmed desorption

Feed mixtures

- NO_2 (1000 ppm)
- NO_2 (1000 ppm) +O_2 (3%)
- NO (1000 ppm)
- NO (1000 ppm) +O_2 (3%)

Catalytic systems

- $Pt/Ba/Al_2O_3$
- Ba/Al_2O_3
- Pt/Al_2O_3

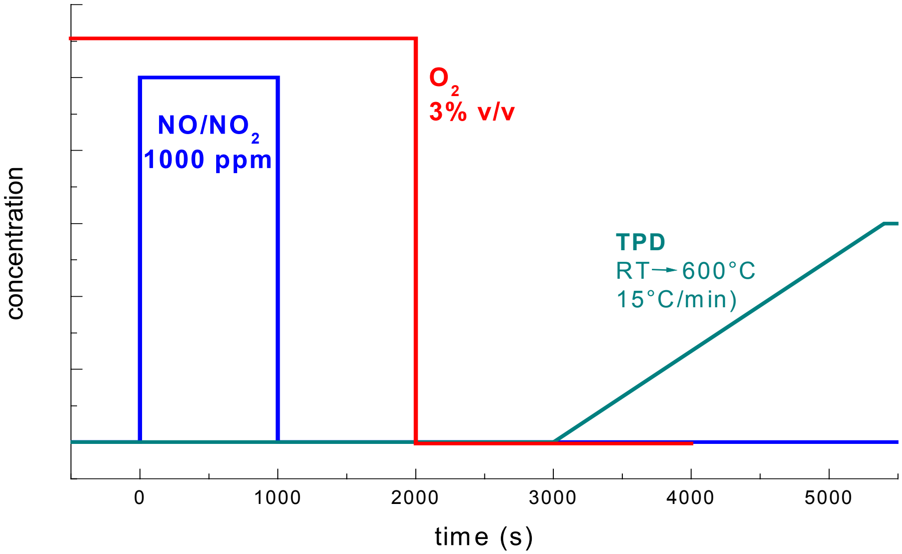

Simulation of the experimental micro- reactor

- **Simulation of the experimental microreactor with a plug – flow non stationary heterogeneous model**

  - Bed density = 0.7 g/cc; Void fraction ~ 0.35
  - Flow ~ 200 Ncc/min; catalyst mass ~ 0.12 g

→ **Space Velocity**: **~10^5 Ncc/g/h**

- Pt load=1%; Ba load=16.7%
- Pt and Ba dispersions: *fitted by non linear regression*

→ Active Pt e Ba moles

- **Hypothesis**
  - Neither internal nor external diffusional resistances
  - No axial dispersion

$$\varepsilon \frac{\partial C_i}{\partial t} = -\frac{\varepsilon}{\tau}\frac{\partial C_i}{\partial \bar{x}} + \Omega_{Pt}\sum_{j=1}^{NR_{Pt}} \nu_{ij} r_j + \Omega_{Ba}\sum_{k=1}^{NR_{Ba}} \nu_{ik} r_k$$

$$\frac{\partial \vartheta_i}{\partial t} = \sum_{j=1}^{NR} \nu_{ij} r_j$$

θ_i= Pt, Ba species

Feed mixture: NO_2 **System:** Ba/Al_2O_3

Experiment

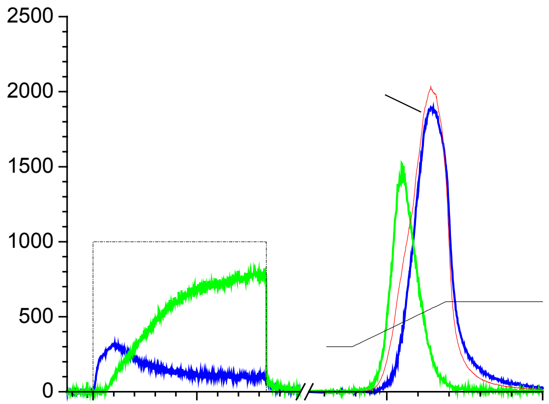

Simulation

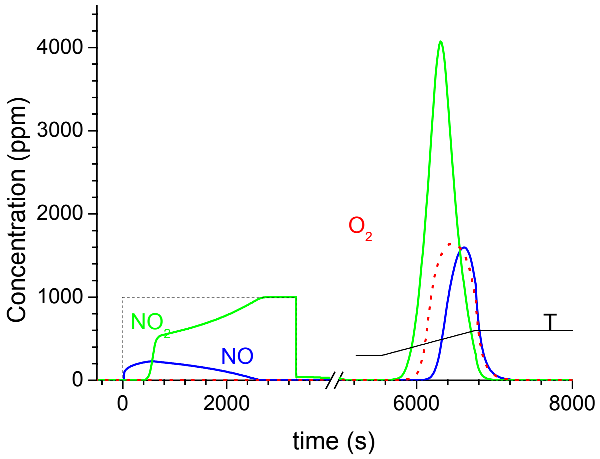

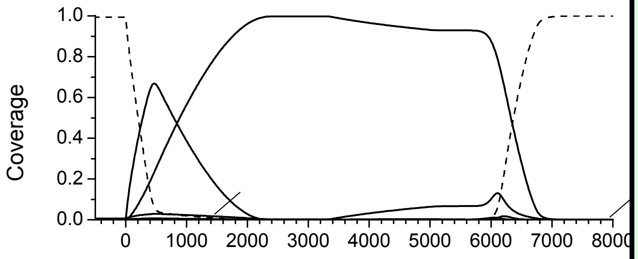

- **S-NO_2 (NITRITES) decomposition = RDS toward NITRATES formation**

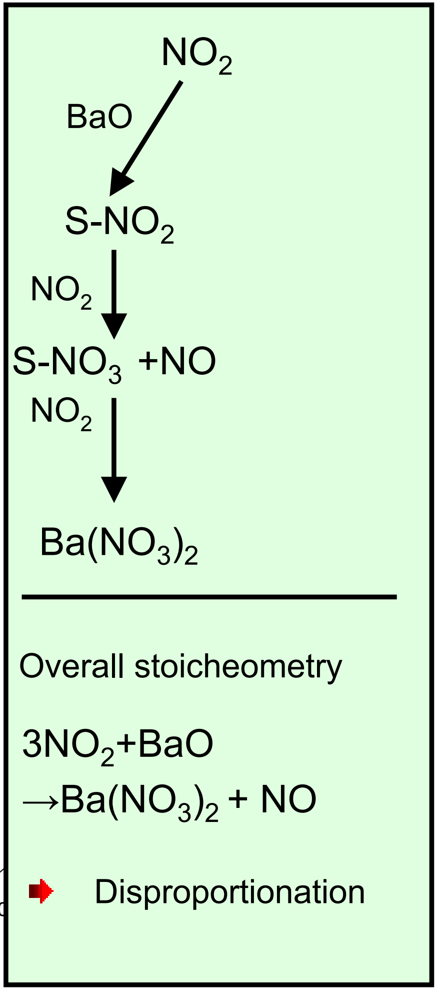

NO_2

BaO

S-NO_2

NO_2

S-NO_3 +NO

NO_2

$Ba(NO_3)_2$

Overall stoicheometry

$3NO_2+BaO$
$\rightarrow Ba(NO_3)_2 + NO$

➧ Disproportionation

Feed mixture: NO_2 System: $Pt/Ba/Al_2O_3$

Experiment

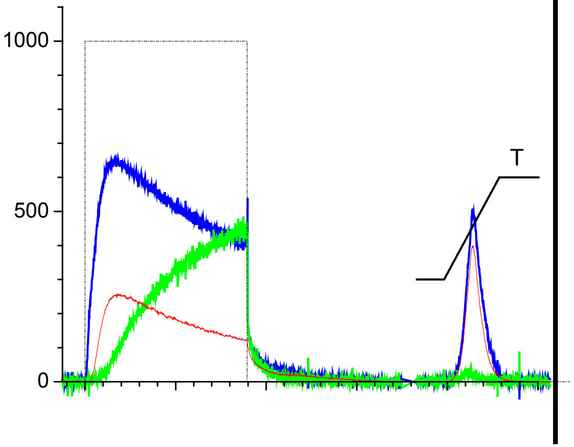

Simulation

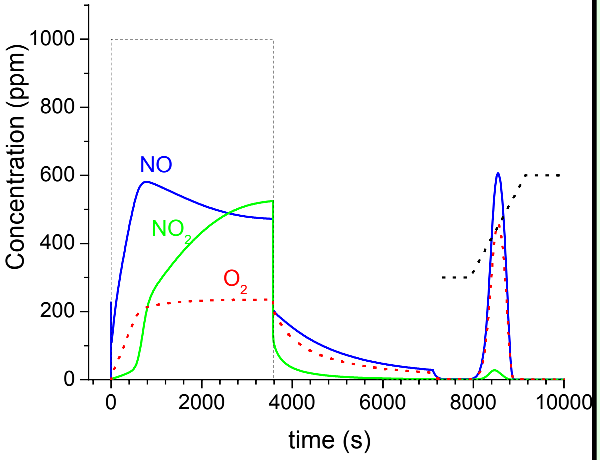

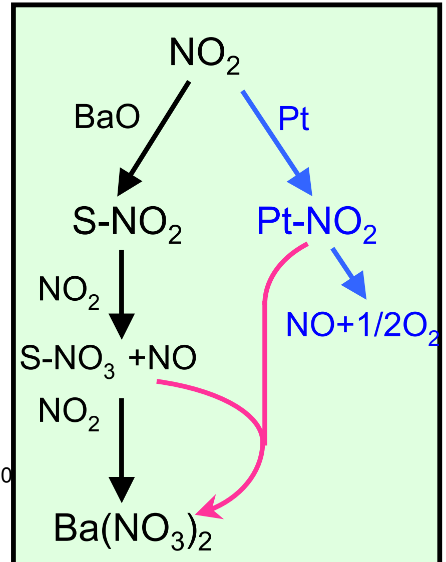

NO_2

BaO

Pt

S-NO_2

Pt-NO_2

NO_2

$NO+1/2O_2$

S-NO_3 +NO

NO_2

$Ba(NO_3)_2$

- Disproportionation
- NO_2 decomposition over Pt

According to the model Pt catalyses these reactions:

- **$NO_2 \rightarrow NO+1/2O_2$: higher outlet concentrations of NO**
- **Spillover reaction, in competition with the formation of nitrates via gas – phase**

Transient kinetics of NOx storage: Conclusions

The kinetic model has been tested in a wide experimental range of:

- feed mixtures
- catalytic systems

Its predictions are useful in identifying the roles of catalyst components and of reacting species:

Role of gas – phase species

- NO_2 is the key species for NOx storage
- O_2 has a role in the presence of Pt, feeding NO or NO_2, involving a dead time both for NO and NO_2

Role of surface species

- Main Barium species: S-NO_2 (nitrites) and $Ba(NO_3)_2$ (nitrates)
- The storage involves a ***two – step disproportionation, with a*** nitrites to nitrates ***slow*** evolution for all the experiments where storage takes place (IR data seem to suggest a different kinetic of evolution of nitrites to nitrates)
- Pt sites oxidize NO ⇔ NO_2

2. Lab-scale structured reactors for kinetic measurements in catalytic combustion

2.1 Structured Annular Reactor for investigation of High Temperature Kinetics of CH_4 Combustion over very active PdO-based Catalysts

- Design of the annular reactor by mathematical modeling
- Experimental performances of the annular reactor
- Kinetics of CH_4 combustion over PdO/ZrO_2 (10% w/w of Pd) catalyst

Kinetic measurements in catalytic combustion

- **Demanding task**
  - Wide temperature ranges are relevant to practical applications (e.g. 350-850°C for G.T.);
  - Extremely fast reactions in the high-T range which are typically affected by diffusion limitation
  - Onset of temperature gradients associated with highly exothermic combustion reactions (high fuel concentration)
  - Industrial applications typically require structured monolith catalysts

Annular flow microreactor

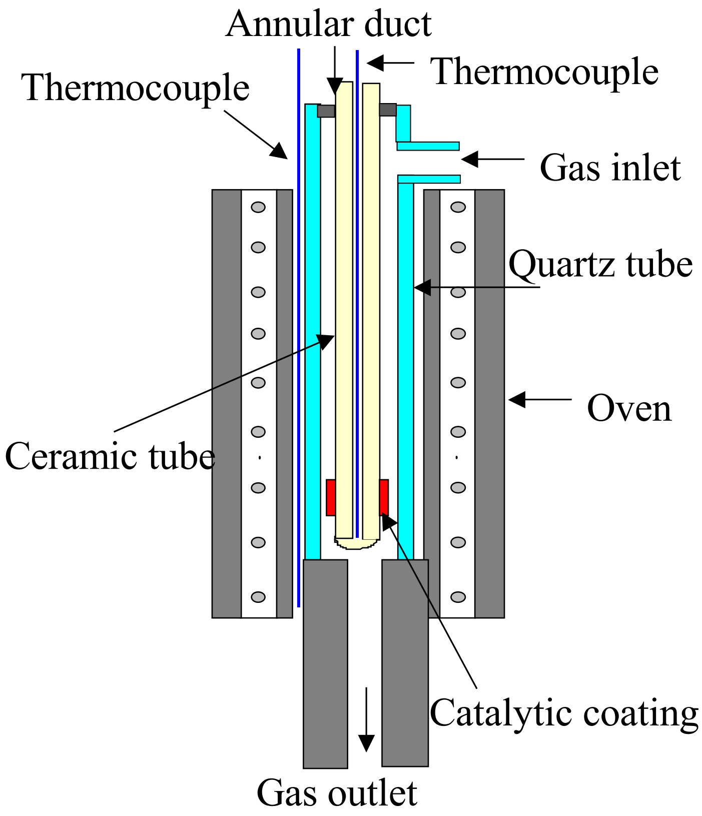

- High GHSV with minimum pressure drop
- Partial conversion at high reaction rate (high T)
- Well defined geometry (and flow pattern) ⇒ assessment and control of diffusional effects
- Effective dissipation of the heat of reaction (radiation)

J. Mc Carty, Catal. Today, 1995
A. Beretta et al. , Appl. Catal. A:Gen., 1999

Annular microreactor: Modeling Assumptions

- Steady state
- Fully developed laminar flow
- 1D lumped description of the gas phase
- 2D description of the catalyst phase
- Isothermal conditions
- Negligible pressure drop
- Planar geometry of the catalyst layer ($r_i/\delta_w>50$)

Governing equations

Gas phase mass balance of f-species

$$u\frac{\partial C_{f,g}}{\partial z}-\left[\left(D_{m,f}+D_{ea,f}\right)\frac{\partial^2 C_{f,g}}{\partial z^2}\right]=\frac{4}{d_h}\left[\frac{\left(r_i+\delta_w\right)}{r_0+\left(r_i+\delta_w\right)}\right]K_{g,f}\left(C_{f,w}-C_{f,g}\right)$$

Catalyst phase mass balance of f-species

$$D_{e,f}\frac{\partial^2 C_{f,w}}{\partial n^2}+\nu_f R_{f,w}=0$$

Boundary condition

$u\left(C_{f,g}-C_{f,g}^{\circ}\right)=\left(D_{m,f}+D_{ea,f}\right)\frac{\partial C_{f,g}}{\partial z}$ inlet condition (at z=0)

$\frac{\partial C_{f,g}}{\partial z}=0$ outlet condition (at z=L)

$D_{e,f}\frac{\partial C_{f,w}}{\partial n}=K_{g,f}\left(C_{f,g}-C_{f,w}\right)$ at catalyst surface (n=δ_w)

$\frac{\partial C_{f,w}}{\partial n}=0$ at catalyst/α-A_2O_3 interface (n=0)

Reactor design

Design parameters:

Catalyst layer thickness (δ_w), annular chamber height (δ_a)

Catalyst and reactor efficiencies (design targets)

$$\eta_{\text{int}}^{av} = \int_0^L \frac{\int_0^{\delta_w} R_w(z,n)\,dn}{R_w(z,\delta_w)\delta_w} dz / L$$ internal catalyst efficiency

$$\eta_{glob} = K_r^{eff} / K_r$$ global reactor efficiency

K_r^{eff} has been calculated using the following simple model:

$$u\frac{dC_{f,g}}{dz} + \frac{(r_i + \delta_w)^2 - r_i^2}{r_0^2 - (r_i + \delta_w)^2} R_{f,w}^{eff} = 0$$ Mass balance of f-species

$$C_{f,g} = C_{f,g}^{\circ}$$ inlet condition

Kinetics $$R_w = \left(\frac{K_r C_{CH_4,w}}{1 + K_{H_2O} C_{H_2O,w}} \right)$$

Overall effectiveness factor

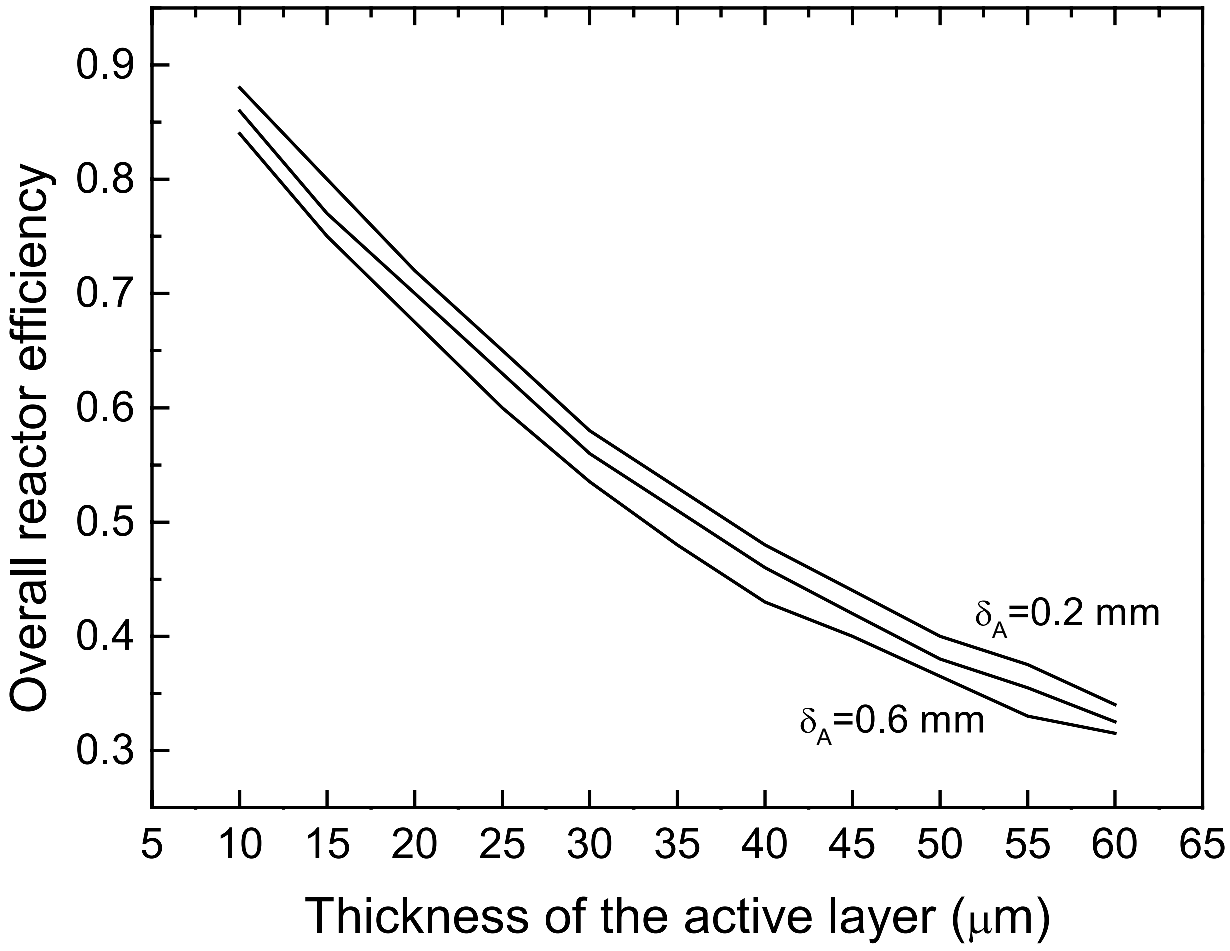

Experimental

- Reactor geometry
  - Structured support: dense α-Al_2O_3 tube
  - r_i=3.25 mm r_o=3.5 mm L_{tot}=80 mm $L_{catalyst}$=10 mm

- Active catalyst layer

Precursor powders

  - PdO/ZrO_2 (10% w/w of Pd) dry impregnation with $Pd(NO_3)_2$ solution

Washcoat deposition (critical step)

  - Dipping the support in a slurry prepared by ball milling precursor powders in a HNO_3 aqueous solution

δ_w=15 µm (6 mg) by SEM and weight measurements (T_c=800°C)

- Investigated ranges of operating variables
  - T=400-550°C; GHSV=10^6 cm^3/gh (@STP)
  - CH_4=0.8-3. 0%; H_2O=0-3.5 %; CO_2=0-2.7% ; O_2=10-20 %

Effect of carrier gas

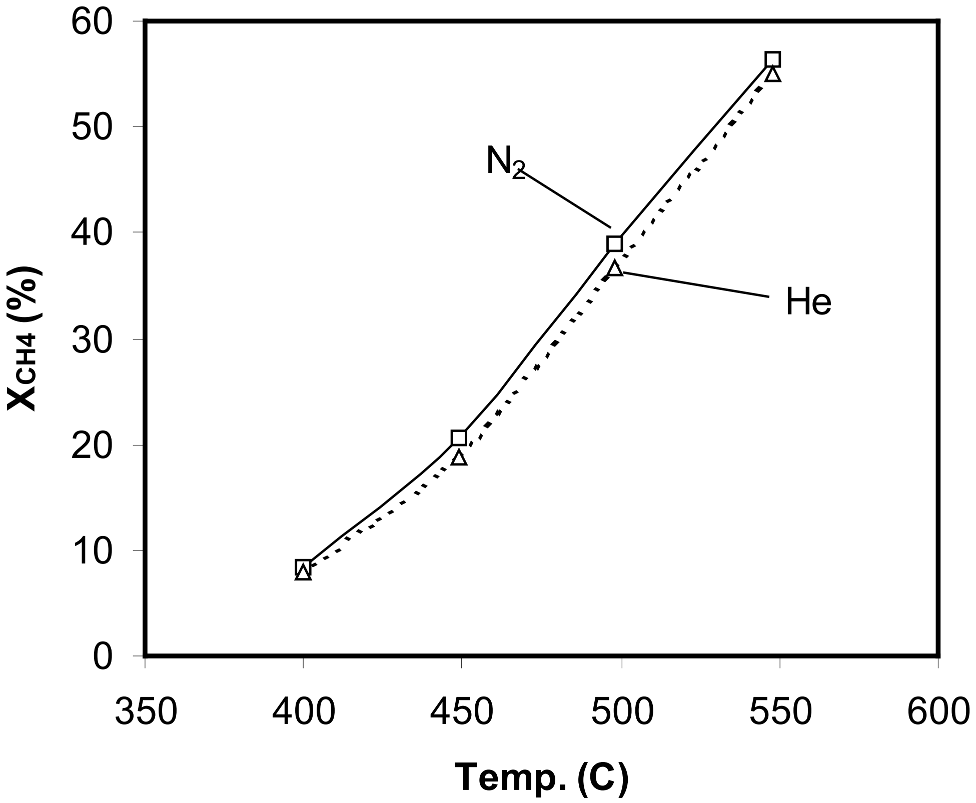

- Negligible diffusional limitations
- Partial conversion has been obtained up to 550°C

Thermal behaviour-1

CH_4 combustion experiments

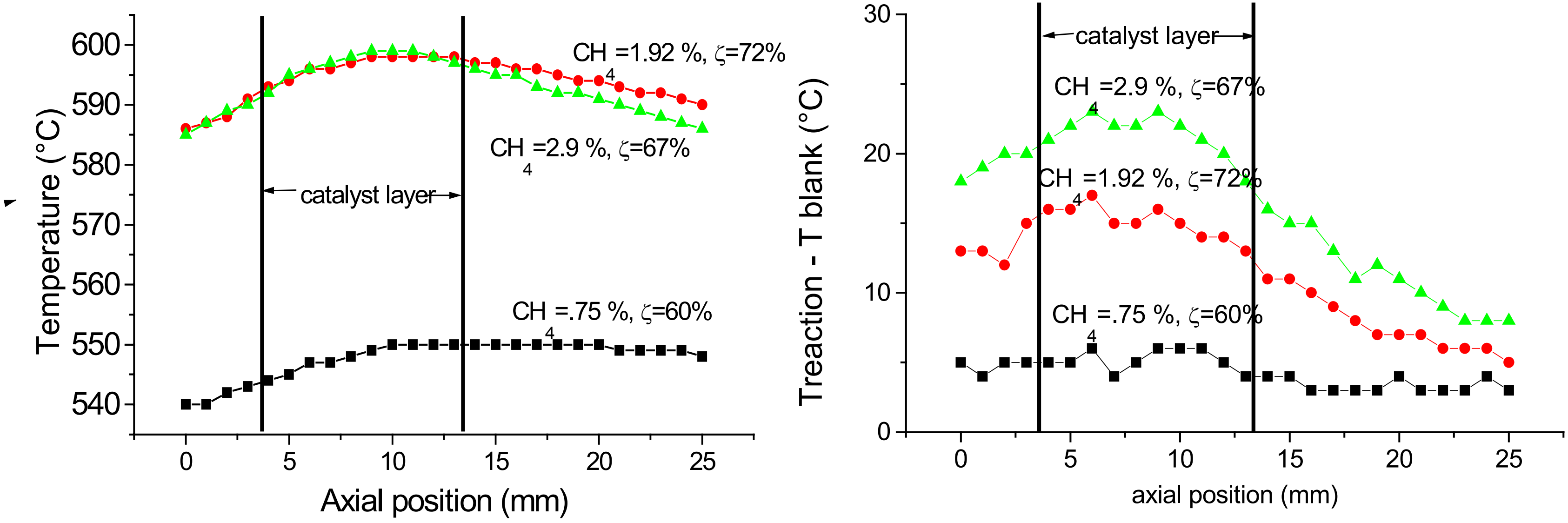

Effective dissipation of reaction heat results in an almost isothermal catalyst layer

Thermal behaviour-2

CO-H_2 combustion tests (CO=4%, H_2=4%)

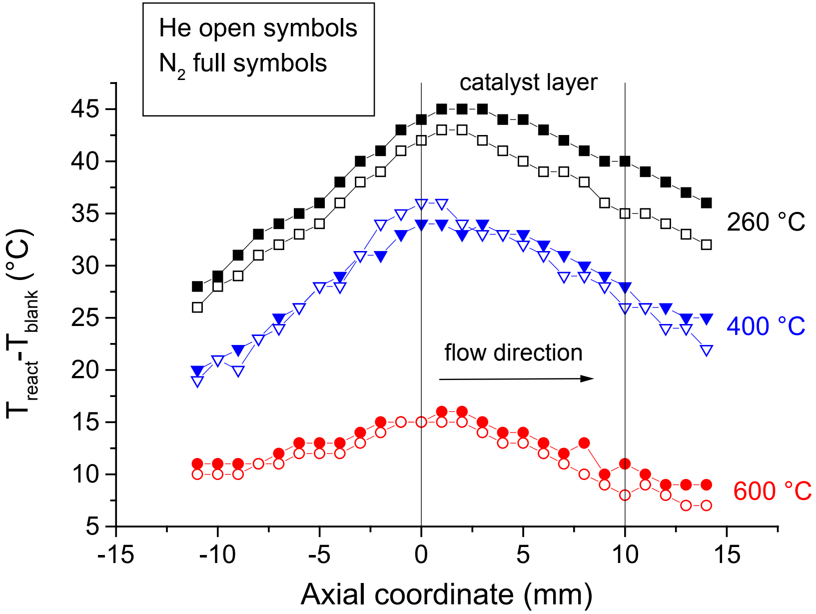

Mechanisms of heat dispersion:

radiation at high T (more effective) convection at low T.

Effects of reactant concentrations

O_2

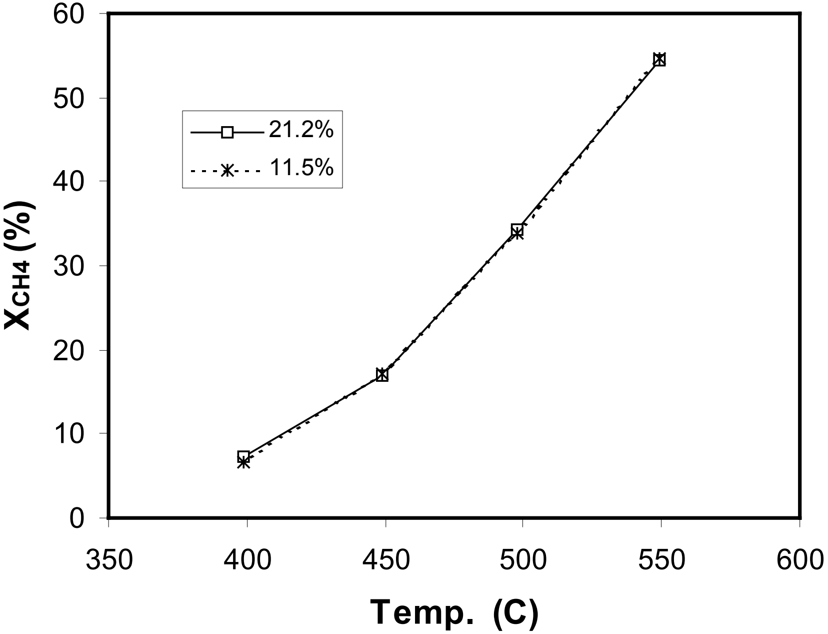

CH_4

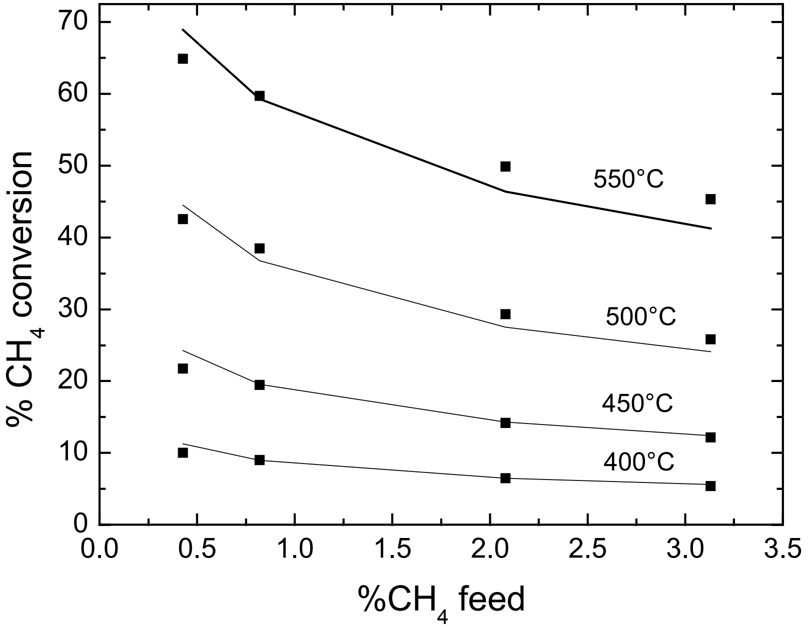

0^{th} order in O_2 concentration
(lean conditions)

Effects of product concentrations

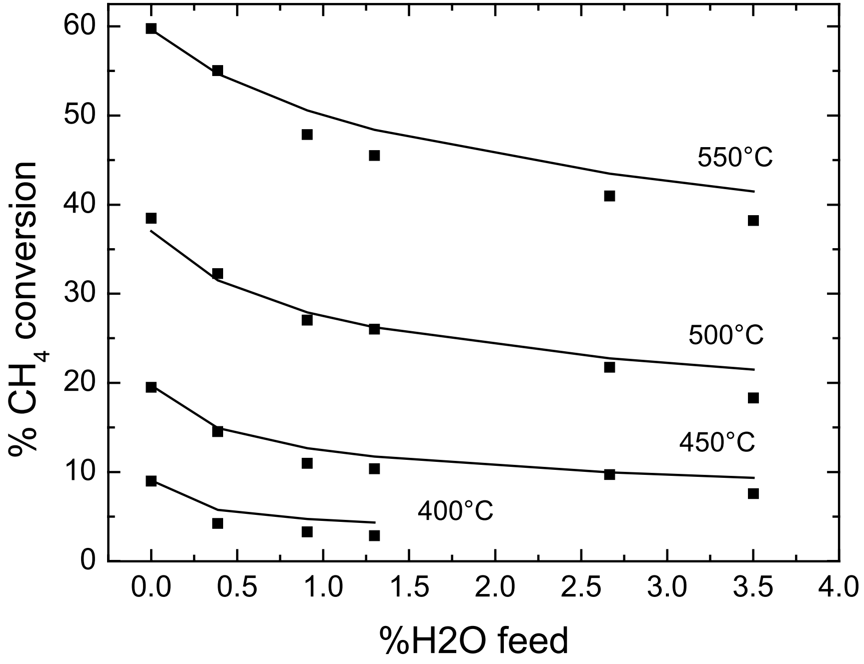

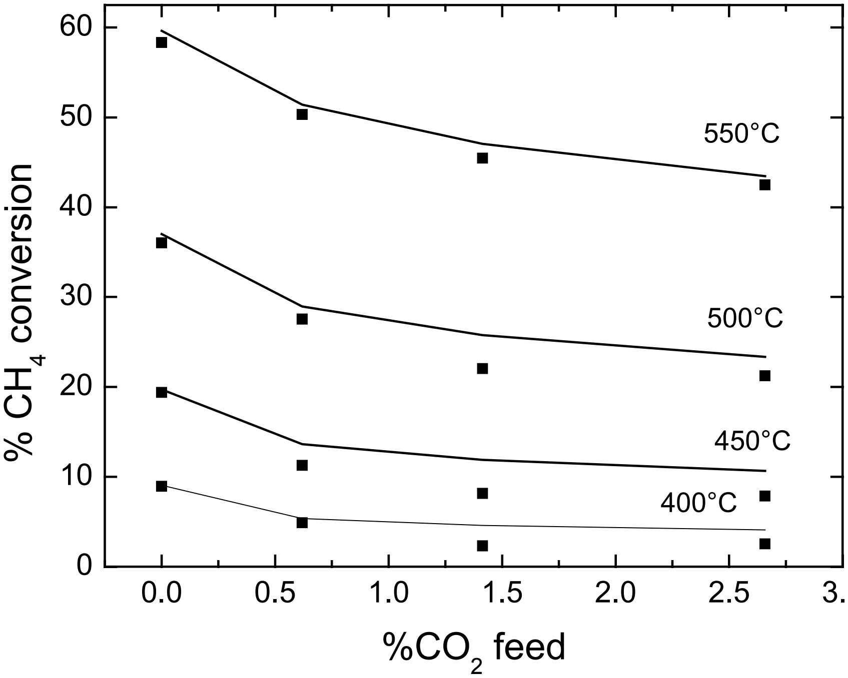

Power law Kinetics: $r = k_r C_{CH4} C_{H2O}^{\beta} C_{CO2}^{\gamma}$

E_{act}=108 kJ/mol; β=-0.32; γ=-0.25

Role of the support on H_2O and CO_2 inhibition

PdO/ZrO_2

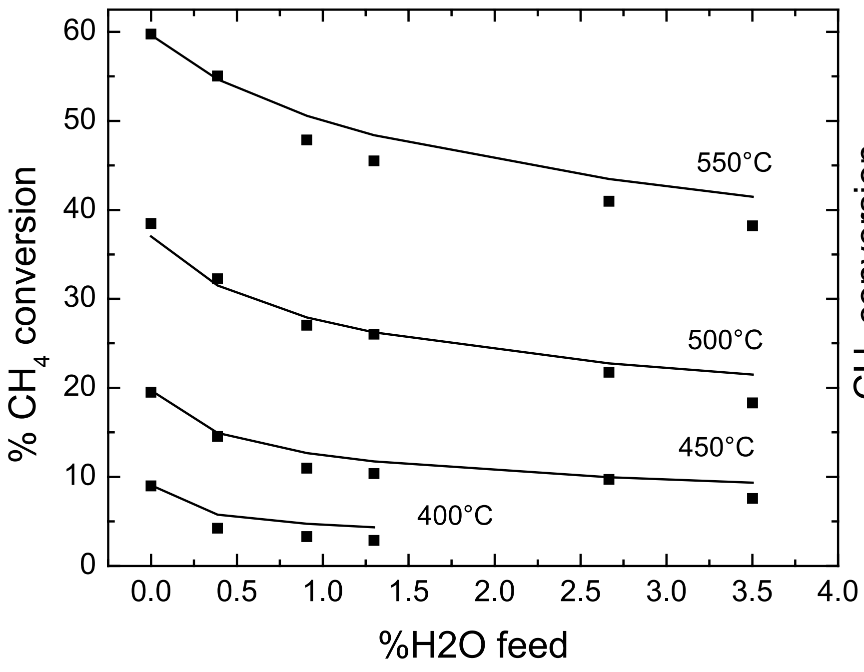

GHSV=10^6 cm^3/gh

PdO/Al_2O_3

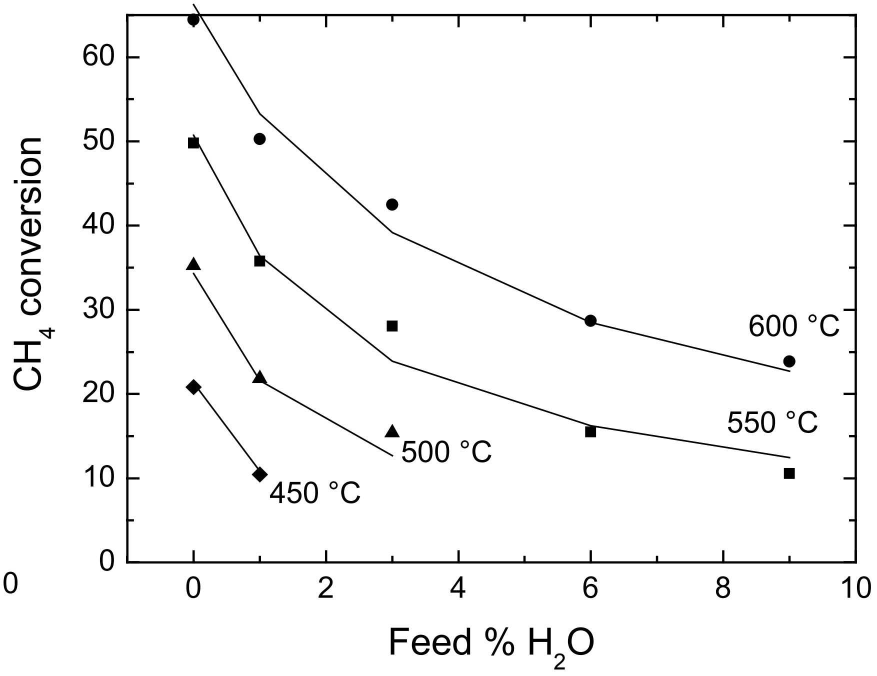

GHSV=3x10^6 cm^3/gh

CO_2 inhibition was not observed up to 10% CO_2 over PdO/Al_2O_3

CH_4 combustion in annular reactor - Conclusions

- A specifically designed annular reactor has allowed to investigate the kinetics of CH_4 combustion over PdO/ZrO_2 (10% Pd w/w) in a 400-550 °C T-range with:
  - minimum impact of diffusional limitations (δ_w=15μm)
  - nearly isothermal conditions (radiation)

- The results of the kinetic study indicated that under the investigated conditions both H_2O and CO_2 similarly inhibit the reaction rate up to 550° C.

- Indications on a primary role of the support on the extent of both such inhibition effects have been found

2. Lab-scale structured reactors for kinetic measurements in catalytic combustion

2.2 Metallic Structured Catalysts with High Thermal Conductivity for the kinetic investigation of strongly exothermic G/S reactions

- Investigate experimentally the <u>thermal</u> behavior of structured metallic catalysts in the presence of a strongly exothermic G/S reaction (CO oxidation)
- Demonstrate the influence of catalyst design parameters
  - support material and geometry
  - coating formulation
- Develop an engineering analysis of the experimental results
  - kinetics
  - thermal resistances

Structured catalysts in non-adiabatic g/s reactors

- Potential advantages:

  + reduced pressure drop
  + easy scale-up
  + **favourable heat transfer properties** due to heat conduction in the connected matrix

Preparation of structured test catalysts - 1

- Supports consisting of four slabs assembled to form 3 parallel rectangular channels
- Catalyst (L = 200 mm) loaded into a rectangular (50x30 mm) reactor tube in an oven with air recirculation
- Five 1/16” tubings glued on the slabs to act as thermowells
- Front view:

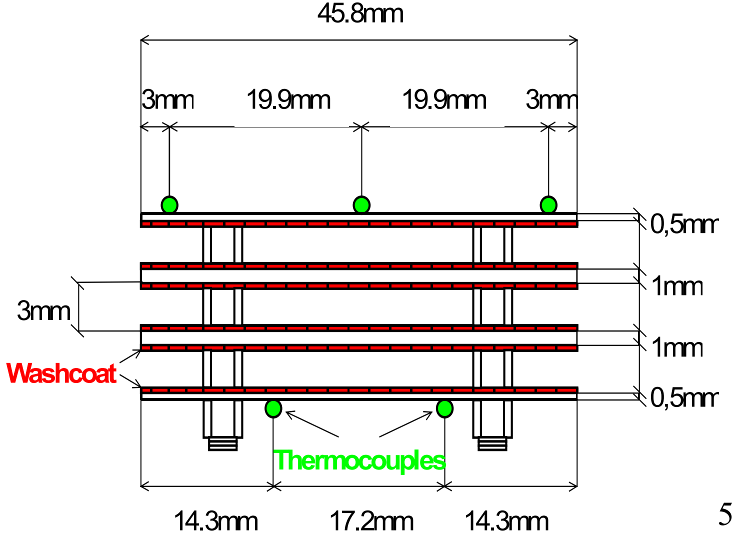

Preparation of structured test catalysts - 2

- Three samples with supports made of
  - Aluminium: $k_{sol} = 200$ W/(m K), s = 0.5 mm **Sample A**
  - AISI 304: $k_{sol} = 20$ W/(m K), s = 0.5 mm **Sample B**
  - AISI 304: $k_{sol} = 20$ W/(m K), s = 0.2 mm **Sample C**
- Washcoated by deposition of 3% Pd/γ-Al_2O_3 (19% w/w) dissolved in sodium silicate
- **Sample D** (Al, s=0.5 mm) precoated with a pseudo-bohemite primer, dipped into a 3% Pd/γ-Al_2O_3 silica-free slurry and flash-dried at 280 °C

CO oxidation runs: Kinetic study

- Investigated ranges, Sample A:

  $Y°_{CO} = 0.02 - 0.09$

  $Y°_{O2} = 0.05 - 0.20$

  $T = 150 - 250 °C$
- Isothermal conditions, no diffusional limitations
- Negative CO reaction order
- Rate expression [moles/m²/s]:

$$r_{CO} = \frac{k_1 p_{CO} p_{O2}^{1/2}}{(1 + k_2 p_{CO})^2}$$

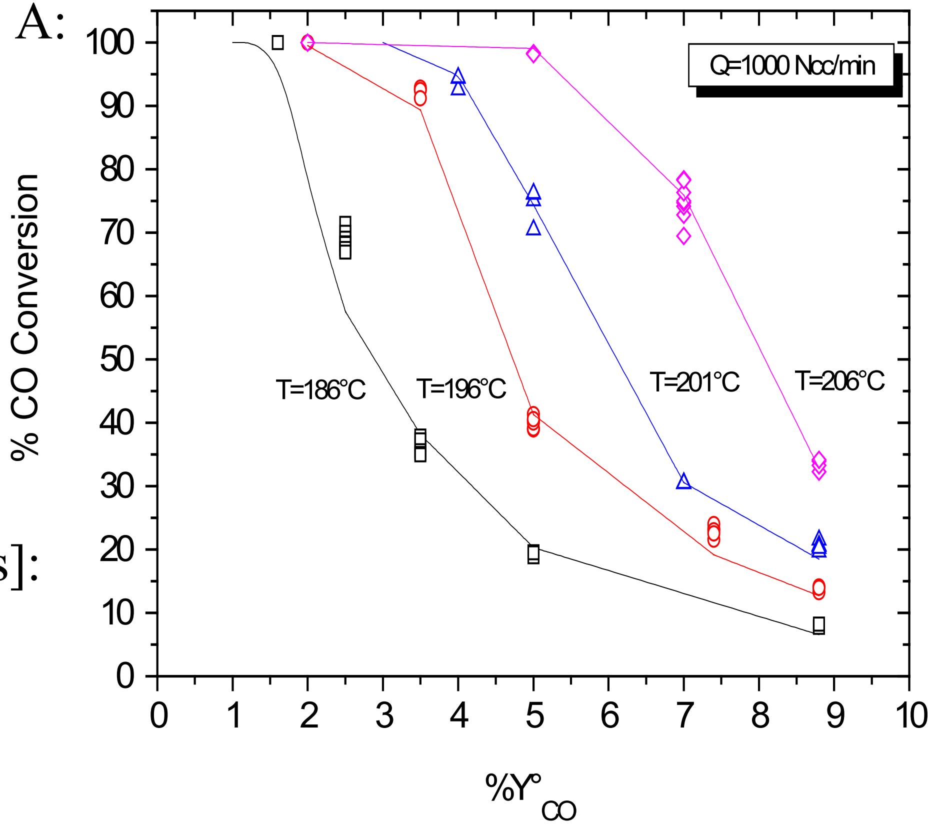

CO oxidation runs: Thermal behavior - 1

- **Al support (sample A):** influence of Toven:

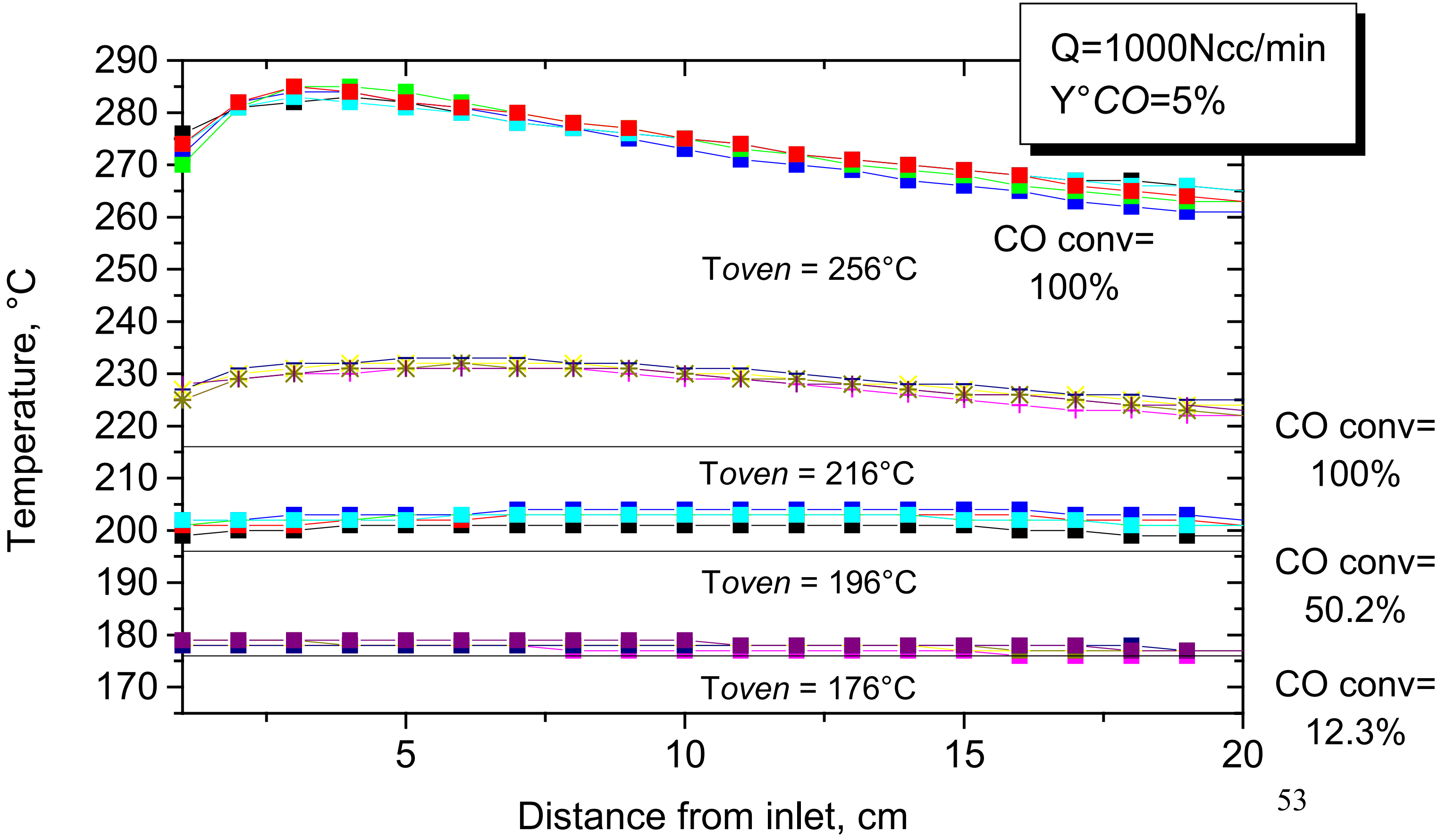

CO oxidation runs: Thermal behavior - 2

- Comparison of Al and Steel supports (s = 0.5 mm):

  Al: k_{sol} = 200 W/(m K) vs. Steel: k_{sol} = 20 W/(m K)

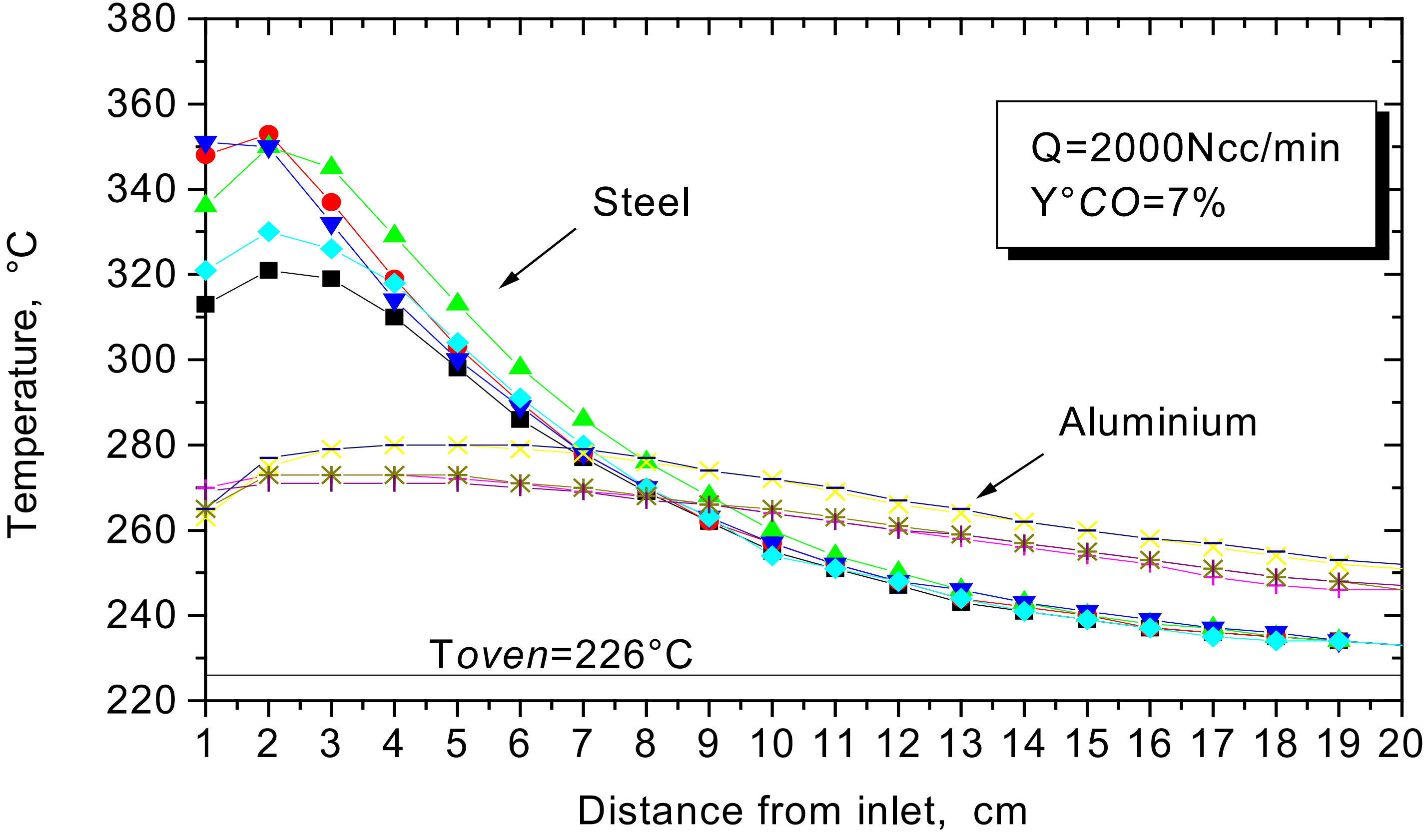

CO oxidation runs: Thermal behavior - 3

- Influences of support material and slab thickness:

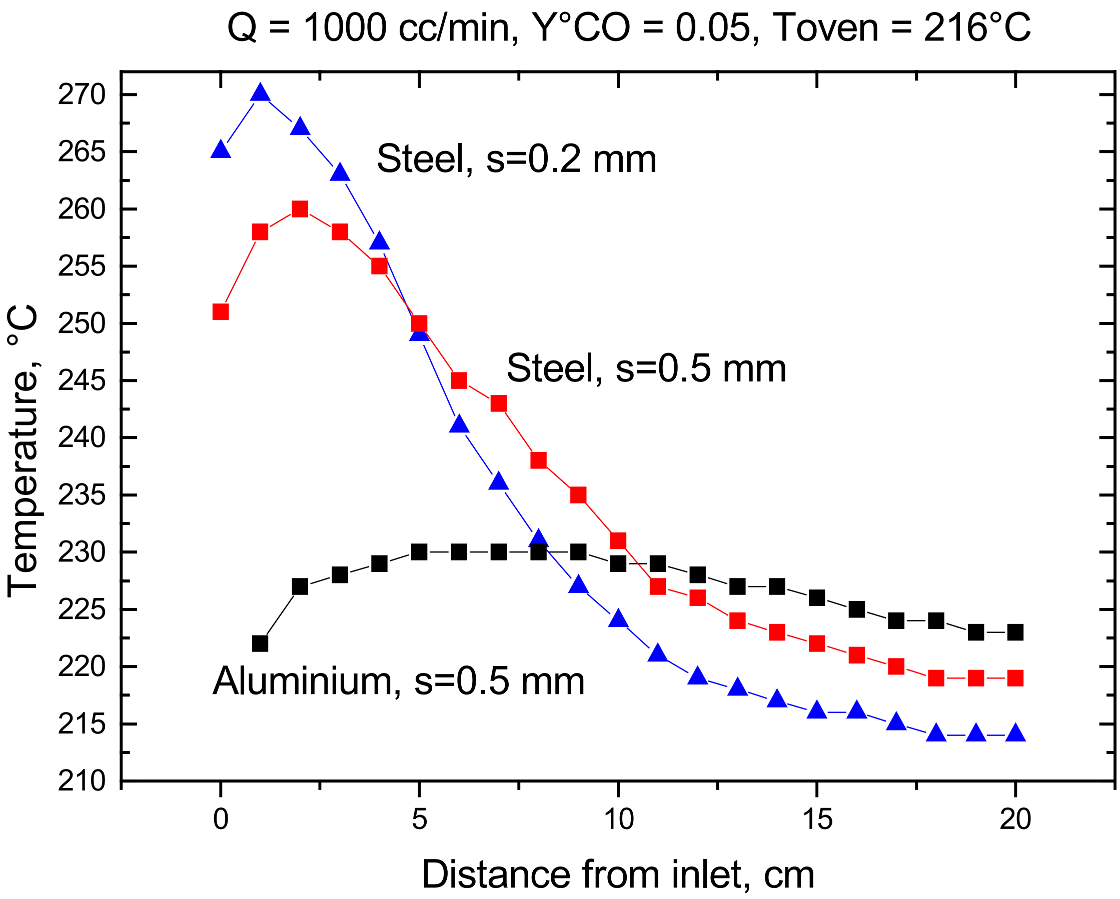

CO oxidation runs: Thermal behavior - 4

- Comparison of lab-scale reactors:

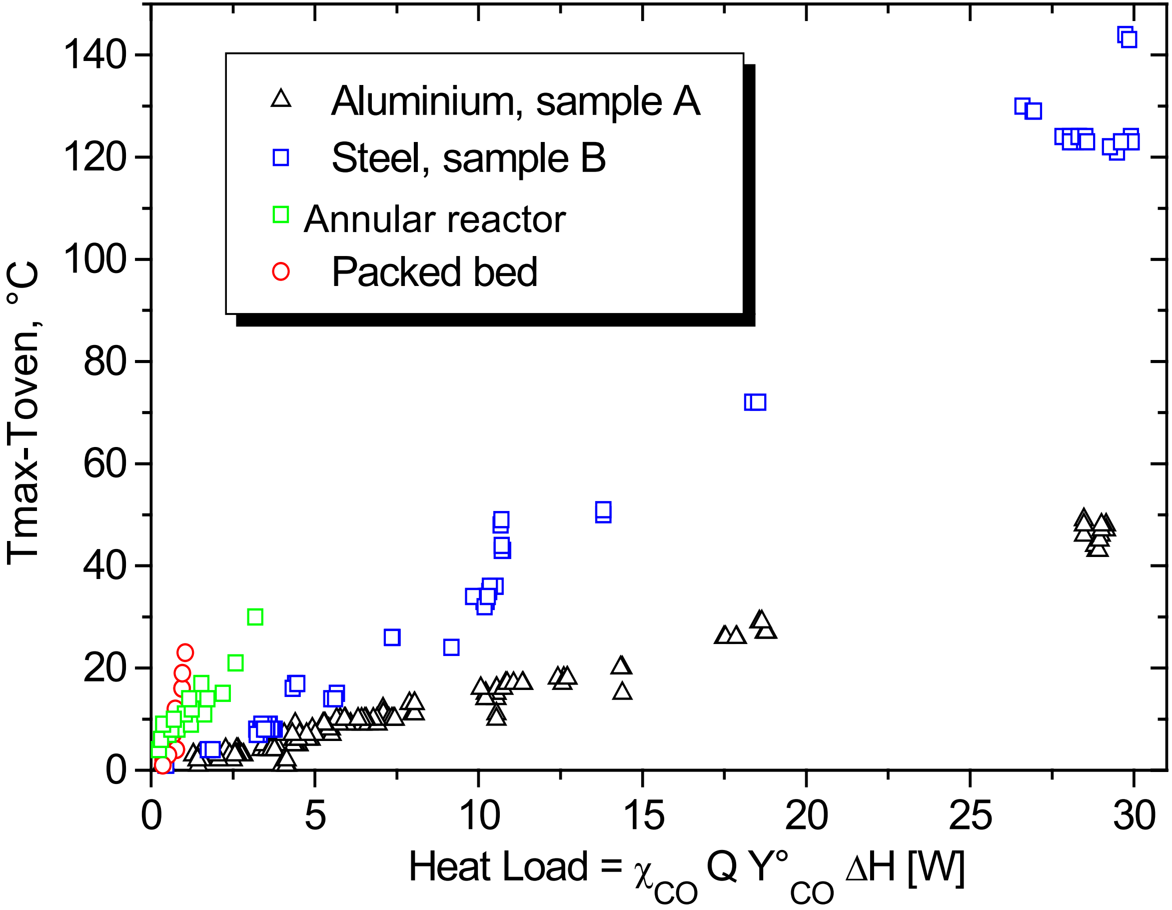

Catalytic activity of Sample D vs. Powders in CO oxidation

data are CO_2 productivities (g CO_2/g_{cat}/h)

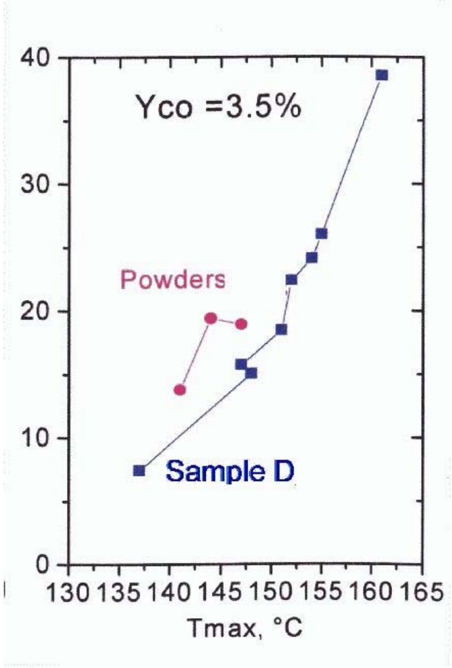

Engineering analysis: Data fit

- Regression results on T-profiles, Sample A:

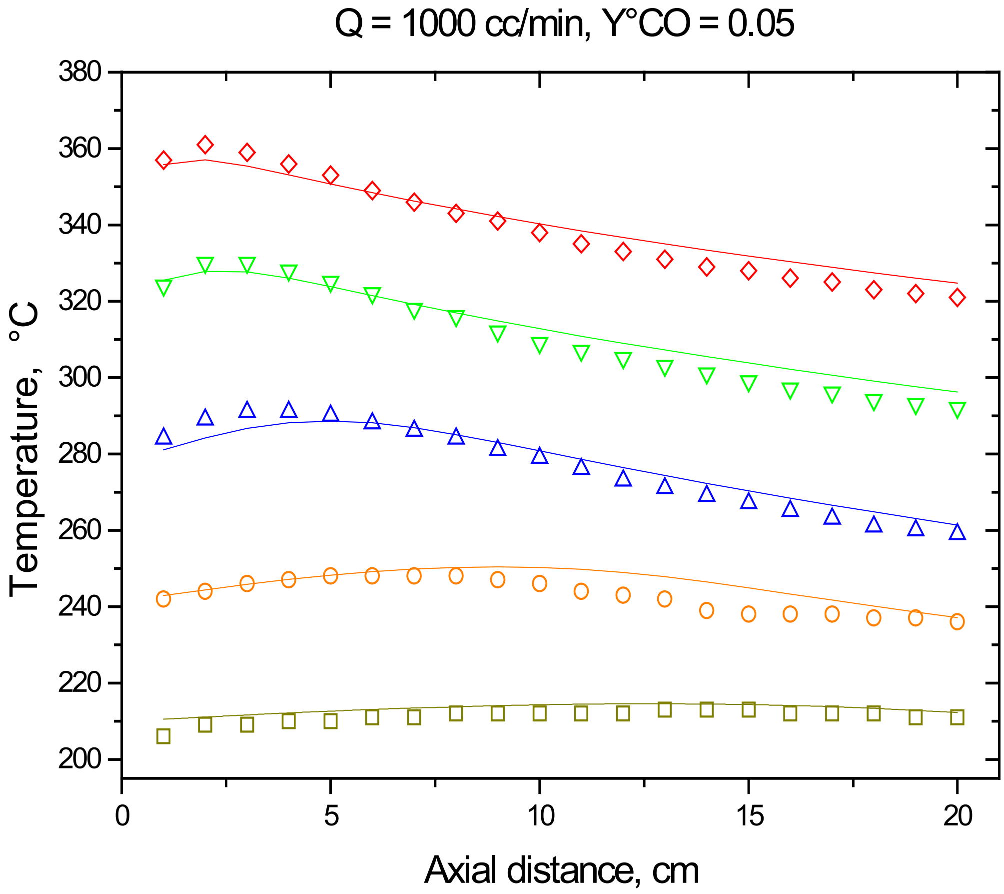

<== Influence of T_{oven}:

1D heterogeneous reactor model;

kinetics from independent isothermal study;

model adaptive parameters are thermal resistances only.

High Conductivity Structured Catalysts: Conclusive remarks

- Heat conduction in the supports of structured metallic catalysts can be exploited to remove effectively the heat of reaction.
- Thermal conductivity and thickness of the support material are critical → catalyst design.
- In the case of highly conductive supports (Al),
  - isothermal runs are possible over wide ranges of operating conditions
  - heat transfer resistances at the catalyst/reactor interface become controlling.
- Results are of interest in view of applications to lab-scale microreactors for kinetic studies

Structured catalysts for catalytic combustion kinetics: main literature references

G. Groppi, E. Tronconi
"Continuous versus discrete models of nonadiabatic monolith catalysts",
AIChE Journal 42, 2382-2387 (1996).

G. Groppi, E. Tronconi, P. Forzatti
“Mathematical models for catalytic combustors”
Catalysis Reviews - Sci.Engng., 41(2), 227-254 (1999).

E. Tronconi, G. Groppi
”A study on the thermal behavior of structured plate-type catalysts with metallic supports for gas/solid exothermic reactions”
Chem. Eng. Sci., 55, 6021-6036 (2000).

G. Groppi, W. Ibashi, E. Tronconi, P. Forzatti
“Structured reactors for kinetic measurements under severe conditions in catalytic combustion over palladium supported systems”
Catal. Today, 69, 399-408 (2001).